

FORET Arnaud

Master Sciences de l'eau

Integrated Watershed Sciences specialization track

June 2025



## Spatial Characterization of Riparian Corridors in the Loire Basin: Integrating LiDAR, GIS, and Multi-Scale Indicators



Partner: SAGE Loire en Rhône-Alpes,  
Supported by the Loire Département,  
Represented by Amélie POTIGNON



Professional tutor: MAZAGOL, Pierre-Olivier

Academic tutor: LANDON, Norbert

Examinator: LEJOT, Jérôme



# Spatial Characterization of Riparian Corridors in the Loire Basin: Integrating LiDAR, GIS, and Multi-Scale Indicators

## 1. Abstract (EN)

Riparian vegetation plays a key role in maintaining river ecosystem functions, especially in the context of increasing climatic and anthropogenic pressures. Monitoring remains spatially inconsistent and methodologically fragmented. This study, conducted as part of a broader research-action initiative within the SAGE Loire en Rhône-Alpes framework, aims to establish a replicable and geomatics-based approach to assess riparian vegetation across varied land uses and hydrological contexts. Using open-access datasets this work implemented workflows for valley bottom delineation, LiDAR-derived vegetation mapping, longitudinal and lateral connectivity analyses, and vegetation quality classification via buffer-based and reach-based matrices. These layers were integrated into a GIS database supporting multi-scalar analysis of vegetation extent, continuity, and density. Results highlight the critical role of high-resolution LiDAR data in detecting narrow or fragmented riparian corridors and underscore the spatial variability of vegetation quality across the watershed. Despite methodological constraints such as segmentation limitations and resolution mismatches, the workflow provides a scalable framework to support conservation planning and restoration prioritization. This research contributes directly to the development of operational tools for water managers and ecological stakeholders seeking to adaptively manage riparian systems under changing environmental conditions.

## 2. Résumé (FR)

La végétation rivulaire, ou ripisylve, joue un rôle essentiel dans le maintien des fonctions écologiques des écosystèmes fluviaux, en particulier dans un contexte de pressions climatiques et anthropiques croissantes. Son suivi reste spatialement hétérogène et méthodologiquement fragmenté. Cette étude, menée dans le cadre d'une initiative plus large de recherche-action portée par le SAGE Loire en Rhône-Alpes, vise à établir une méthode reproductible basée sur les outils de la géomatique pour évaluer la végétation rivulaire dans des contextes variés d'occupation du sol et de dynamique hydrologique. À partir de jeux de données en accès libre, cette approche a mis en œuvre plusieurs chaînes de traitement : délimitation des fonds de vallée, cartographie de la végétation à partir du LiDAR, analyses de connectivité longitudinale et latérale, ainsi que classification de la qualité de la végétation via des matrices fondées sur des zones tampons et des tronçons de cours d'eau. Ces couches ont été intégrées dans une base de données SIG permettant une analyse multi-échelle de l'étendue, de la continuité et de la densité de la végétation. Les résultats soulignent l'importance cruciale des données LiDAR haute résolution pour la détection des corridors rivulaires étroits ou fragmentés, et mettent en évidence la variabilité spatiale de la qualité de la végétation à l'échelle du bassin. Malgré certaines limites méthodologiques, telles que les difficultés de segmentation et les écarts de résolution, la chaîne de traitement proposée offre un cadre évolutif permettant d'appuyer la planification de la conservation et la hiérarchisation des actions de restauration. Ce travail contribue directement au développement d'outils opérationnels à destination des gestionnaires de l'eau et des acteurs écologiques souhaitant adapter la gestion des systèmes rivulaires face aux changements environnementaux.

**Keywords:** Connectivity analysis, Geographic Information Systems (GIS), LiDAR, Riparian vegetation, Restoration and conservation planning, Valley bottom delineation, Vegetation density



## Table of contents

1. Abstract (EN) .....	3
2. Résumé (FR) .....	3
3. List of Acronyms .....	7
4. Table of Figures .....	8
5. Introduction .....	9
5.1. Riparian vegetation .....	9
5.2. Geomatics in riparian vegetation monitoring .....	10
5.3. Knowledge gaps .....	11
5.4. Benefits of research action .....	11
5.5. Context .....	12
5.6. Data Availability .....	13
5.7. Problem Statement .....	13
5.7.1. Objectives .....	13
5.7.2. Hypotheses .....	13
6. Study Area .....	14
7. Material and methods .....	15
7.1. Valley bottom .....	15
7.2. Vegetation delineation .....	18
7.3. Longitudinal continuity .....	20
7.4. Vegetation Density .....	20
7.5. Lateral Continuity .....	22
7.6. Evaluation Matrix .....	23
8. Results .....	25
8.1. Valley Bottom Delineation .....	25
8.2. Vegetation Delineation .....	26
8.3. Longitudinal Continuity .....	27
8.4. Vegetation Density .....	28
8.5. Lateral Continuity .....	29
8.6. Potential quality evaluation matrix .....	30
9. Discussion .....	32
10. Limits .....	33
11. Perspectives .....	34
12. Conclusion .....	35

13.	Acknowledgments .....	36
14.	References .....	37
15.	Appendix.....	41
15.1.	Appendix 1: DEM Detail .....	41
15.2.	Appendix 2 : RGE Alti DEM Data Sources .....	42
15.3.	Appendix 3: DEM of Difference between LiDAR and RGE Alti.....	43
15.4.	Appendix 4: In situ validation for vegetation density.....	44
15.5.	Appendix 4: R script: DEM from LiDAR.....	45
15.6.	Appendix 5: R script: Tree top extraction.....	46
15.7.	Appendix 6: Python scripts for the evaluation matrix.....	48

### 3. List of Acronyms

ALS	Airborne Laser Scanning (used interchangeably with LiDAR)
BD	Base de Données (Database, often refers to IGN datasets like BD TOPO, BD ORTHO)
CHM	Canopy Height Model
DEM	Digital Elevation Model
DTM	Digital Terrain Model
FCT	Fluvial Corridor Toolbox (GIS plugin for river valley analysis)
GIS	Geographic Information System
GPS	Global Positioning System
GRASS	Geographic Resources Analysis Support System (an open-source GIS software)
HD	High Definition
IBC-R	Indice de Biodiversité des Corridors Ripisylve (Biodiversity Index for Riparian Corridors)
IGN	Institut Géographique National (French National Geographic Institute)
INRAE	Institut National de Recherche pour l'Agriculture, l'Alimentation et l'Environnement
INSEE	Institut National de la Statistique et des Études Économiques (French National Statistics)
LAS	LASer file format (LiDAR point cloud format)
LAZ	Compressed LAS format (LiDAR)
LRA	Loire en Rhône-Alpes
NDVI	Normalized Difference Vegetation Index
OCS	Occupation du Sol (Land Use)
OCSGE	Occupation du Sol a Grande Echelle (Large Scale Land Use Database by IGN)
ORTHO	Orthophotographie (Orthophoto) Plan d'Aménagement et de Gestion Durable (Sustainable Management and Development Plan)
PAGD	Plan
QBR	Qualitat del Bosc de Ribera (Spanish Riparian Forest Quality Index)
QGIS	Quantum GIS (open-source GIS software)
RGE	Referentiel a Grande Echelle (High Resolution National Map Data by IGN – RGE ALTI)
SAGE	Schéma d'Aménagement et de Gestion des Eaux (Water Development and Management Scheme)
SDAGE	Schéma Directeur d'Aménagement et de Gestion des Eaux (Water Master Plan)
TOPO	Topography
UAV	Unmanned Aerial Vehicle (e.g., drones)
VBET	Valley Bottom Extraction Tool (for delineating valley bottoms in GIS)

## 4. Table of Figures

Figure 1: Ecosystem services of riparian vegetation, with the relation to its water table, modified from McDonald et al., 2018 .....	9
Figure 2: Land cover and geology of the SAGE Loire en Rhone Alpes. Sources: CORINE LAND COVER, BRGM.....	14
Figure 3:Valley bottom delineation process workflow.....	16
Figure 4: Input and output parameters of the valley bottom extraction tool on a cross section of a theoretical river ant associated floodplain. ....	17
Figure 5: Differences between the IGN vector layer and the extracted vegetation layer from the classified LiDAR, with visual comparison .....	19
Figure 6: Formula calibration for the algorithm. Numbers on top of the boxplot are the number of trees detected.....	21
Figure 7: Creation of 500m long riparian buffers along streams. ....	22
Figure 8: Result of the valley bottom delineation, with a zoom on Boen sur <i>Lignon</i> , and compared with the Q100 flood prediction from Loire Forez Agglomération, in charge of this watershed.....	25
Figure 9: Result of the forest delineation from LiDAR, with a zoom on Boen sur <i>Lignon</i> .....	26
Figure 10: Result of the longitudinal continuity analysis, with a zoom on Boen sur <i>Lignon</i> . ....	27
Figure 11: Result of the density analysis by applying the tree top method, with the represented quadrats counted on site, representing three different typologies of forest.....	28
Figure 12: Result of the lateral continuity analysis, here representing the percentage of coverage of buffers by forest, with a zoom on Boen sur <i>Lignon</i> . ....	29
Figure 13: Result of experimental buffer matrix, with a zoom on Boen sur <i>Lignon</i> .....	30
Figure 14: Result of the experimental matrix, displayed this time as lines, with a 500m reaches size, with a zoom on Boen sur <i>Lignon</i> .....	31
Appendix 1: Difference between available RGE ALTI DEM and LiDAR-derived DEM .....	41
Appendix 2: REG ALTI DEM data sources over the study area, showing re-sampled 25m resolution BD ALTI, low resolution lidar data, and winter photogrammetry.. ....	42
Appendix 3: DEM of Difference between the RGE ALTI and the LiDAR-derived DEM .....	43
Appendix 5: 3D view of the place Jean-Jaures in Saint Etienne, used for calibration of the algorithm, with results with the best formula .....	44
Appendix 4: Geolocalised tree count on site in Saint Etienne, compared with the detected trees with the best formula. ....	44
Appendix 6: R script for batch DEM creation from LiDAR data .....	45
Appendix 7: R script fo the batch Tree Top detection using LiDAR .....	47
Appendix 8: Python script used to create the buffered evaluation matrix. ....	48
Appendix 9: Python script used to merge the buffered result to a line result. ....	50



## 5. Introduction

### 5.1. Riparian vegetation

Riparian vegetation refers to the plant communities that occur along watercourses—streams, rivers, and wetlands—occupying the transitional zone between terrestrial and aquatic environments known as ecotones. These communities are shaped by the duration and variability of water presence and are composed of hydrophilic and hydromorphic species adapted to wet or flood-prone conditions. Typically, willows (*Salix spp.*), alders (*Alnus spp.*), and ashes (*Fraxinus spp.*) occupy stream banks, while slightly elevated zones support maples and elms, and upper slopes may feature pedunculate oaks (*Quercus robur*) and hornbeams (*Carpinus betulus*) (Glossaire eau et biodiversité, 2018; Mc Donald et al., 2018).

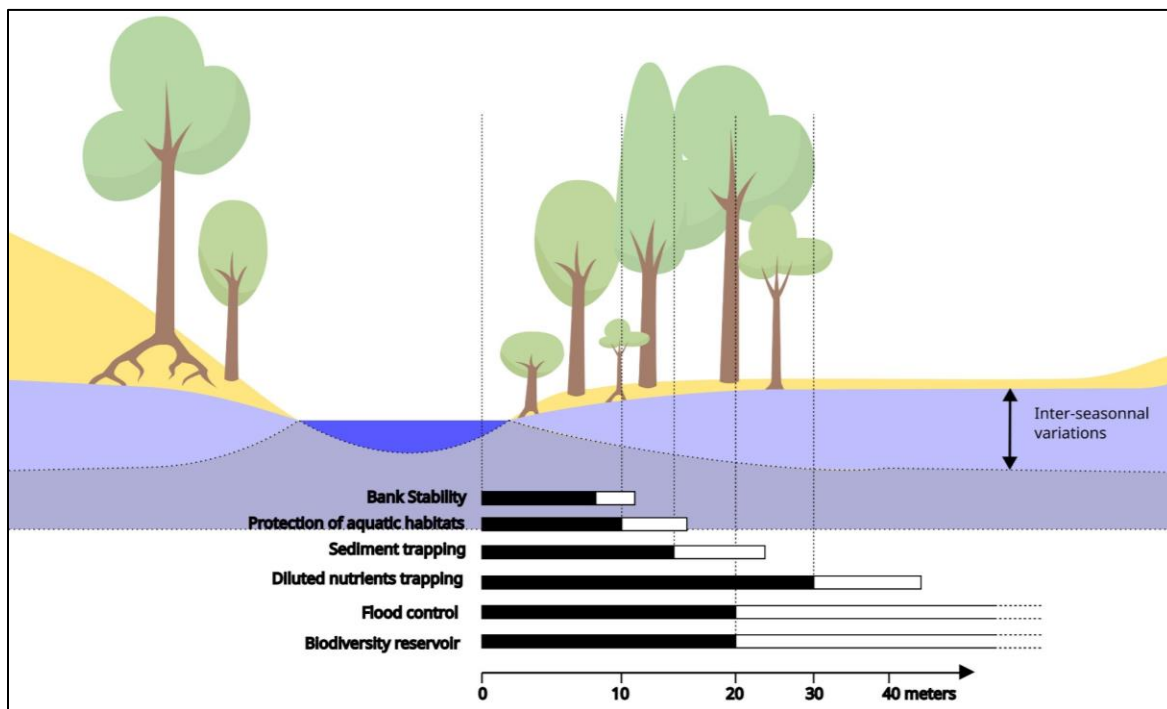


Figure 1: Ecosystem services of riparian vegetation, with the relation to its water table, modified from McDonald et al., 2018

Those riparian zones play a foundational role in the functioning of riverine systems, being at the interface of land and water (Figure 1). It stabilizes banks through root reinforcement, reduces soil erosion, filters sediments and nutrients from runoff, and improves water quality by intercepting pollutants before they reach aquatic environments (Macfarlane et al., 2017; Michez et al., 2017). These areas also regulate stream temperatures through shading, contributing to the thermal balance of aquatic ecosystems—an essential function in the context of rising temperatures driven by climate change (Godfroy et al., 2022; Seavy et al., 2009). Riparian zones also support ecological connectivity by serving as habitat corridors for wildlife and connecting biodiversity across terrestrial and aquatic domains (Capon et al., 2013; Riis et al., 2020). Literature tends to estimate the optimal width of the riparian buffer to around 30 meters (Sweeney & Newbold, 2014).

Beyond their ecological roles, riparian ecosystems are also vital for hydrological regulation, nutrient cycling, and soil fertility. They promote organic matter exchange across the aquatic–terrestrial boundary, supporting productive aquatic food webs (Michez et al., 2017). These services, however, are increasingly under threat. Urbanization, agricultural intensification, hydrological fragmentation, and climate-driven stressors all contribute to riparian degradation (Baatrup-Pedersen et al., 2018; Camporeale et al., 2013).

Climate change exacerbates these pressures by intensifying extreme weather patterns, altering precipitation regimes, and increasing temperature variability. The resulting impacts — such as lower summer flows, higher flood peaks, and increased evapotranspiration — lead to water stress and ecological shifts. Drought-tolerant species may outcompete native flora, while higher water temperatures threaten aquatic organisms relying on shaded habitats (Capon et al., 2013; Dufour et al., 2019). These disruptions also make riparian zones more vulnerable to invasive species and compound the challenges of ecological restoration (Godfroy et al., 2022).

Recognizing these threats, European and national frameworks — such as the Water Framework Directive (European Parliament, 2000), the French SDAGE plans, and the Nature Restoration Regulation (European Union, 2024) — now mandate riparian conservation as a strategic objective. The latest policy aims to restore at least 30% of degraded habitats by 2030, emphasizing the need for spatial tools to identify and prioritize riparian restoration at scale.

## 5.2. Geomatics in riparian vegetation monitoring

Geomatics applications, primarily Geographic Information Systems (GIS), remote sensing, and ALS (Airborne Laser Scanning), such as LiDAR (Laser Infrared Detection And Ranging), have become predominant tools for the study and management of the environment, including riparian vegetation (Godfroy et al., 2022). These approaches enable spatial delineation and modeling of vegetation structures and their interactions with geomorphological and hydrological features. GIS allows for integration of multi-source spatial data to identify vegetation patterns relative to terrain, land use, and water proximity (Sciuto et al., 2022).

Remote sensing platforms, such as high-resolution orthophotos, provide temporal series useful for monitoring vegetation change, especially when integrated with multispectral or hyperspectral imagery. These tools are particularly valuable for identifying phenological cycles, vegetation stress, and long-term degradation patterns in riparian zones (Godfroy et al., 2022; Lochin et al., 2025; Pace et al., 2022). On the other hand, airborne LiDAR captures fine-scale three-dimensional vegetation structures, including canopy height, density, and stratification, even in narrow or densely vegetated corridors (Michez et al., 2017; Roussel et al., 2020; Stackhouse et al., 2023).

Advancements in machine learning, such as object-based image analysis and random forest classification, now enhance the accuracy of riparian vegetation delineation in complex landscapes. These methods can offer robust classification over large extents, outperforming traditional pixel-based approaches in mixed or fragmented environments (Segura-Méndez et al., 2023).

Moreover, open source available tools are spreading within environment domains, enabling more robust analysis of terrain, structures and composition of riparian zones (Gilbert et al., 2016; Grijseels et al., 2021; Macfarlane et al., 2017; Roux et al., 2015).

### 5.3. Knowledge gaps

A major constraint in current mapping efforts is the spatial resolution of widely used remote sensing datasets. Standard 30-meter imagery (e.g., Landsat) fails to capture narrow riparian strips, especially in anthropogenically modified landscapes, where vegetation fragments are often smaller than a pixel or intermixed with agricultural or urban features (Macfarlane et al., 2017). Even with higher-resolution imagery like Sentinel-2 or Pleiades, underestimation of vegetative cover may occur in areas with steep topography or complex canopy shadowing (Lejot et al., 2011).

Riparian zones are highly dynamic, subject to hydrological fluctuations, varied sediment deposition or erosions, and fast vegetation succession (Metz et al., 2016). Yet many mapping efforts rely on single-date observations, limiting the detection of degradation trends or regrowth following disturbance (Breton et al., 2023). While NDVI and LiDAR-derived vegetation metrics can reflect canopy changes, they are rarely updated at temporal scales sufficient to capture intra-annual, even inter-annual variation (Godfroy et al., 2022).

The lack of methodological consistency across riparian mapping studies presents another challenge. Differences in buffer widths, classification thresholds, and delineation tools lead to heterogeneous outputs that are not easily comparable across spatial or administrative scales (Dufour et al., 2019; Segura-Méndez et al., 2023). Even within the same watershed, variation in LiDAR processing or object classification can yield different results for extent, structure, or connectivity of riparian vegetation (Macfarlane et al., 2017).

The limited integration of stakeholder input in the development of geomatics-based monitoring tools is also critical for research. Many outputs are technically robust but lack relevance or accessibility for river managers or conservation planners. This undermines their application in practical settings (Breton et al., 2023). Approaches based on data co-production—where stakeholders contribute to indicator selection, tool development, and ground validation—remain underutilized, despite being shown to improve adoption and utility (Reed et al., 2014).

The integration of hydrological, geomorphological, and ecological data remains limited. Holistic understanding of riparian functionality—particularly under climate change—requires interdisciplinary approaches that combine hydroclimatic models, functional ecology, and land use planning (Dufour et al., 2019; Godfroy et al., 2022). The fragmentation of datasets and analytical workflows continues to hinder the development of scalable, transferable tools.

### 5.4. Benefits of research action

Integrating scientific research with practical land and water management—commonly termed research-action—produces a wide array of benefits for both researchers and practitioners. One of the most impactful outcomes is the co-production of data, which enhances the accuracy,

applicability, and long-term utility of environmental information, particularly in complex, spatially heterogeneous ecosystems like riparian zones.

Data co-produced in collaboration with stakeholders is more likely to reflect local realities, making it directly usable for decision-making and planning. In riparian management, this ensures that spatial indicators (e.g., vegetation extent, continuity) are developed in ways that are both ecologically meaningful and operationally feasible (Reed et al., 2014). Such relevance fosters stronger alignment between monitoring outputs and management needs.

Field validation by local stakeholders improves the spatial and thematic accuracy of geospatial data (Danielsen et al., 2014). Involving practitioners in data acquisition (e.g., GPS marking of features, remote sensing interpretation) allows the correction of misclassifications and enhances the interpretability of geospatial outputs. This collaborative model also leverages tacit ecological knowledge held by local actors.

Engaging stakeholders in the data collection process builds technical capacity and fosters shared ownership of the data infrastructure. This empowerment enables long-term sustainability of monitoring programs, especially in decentralized governance contexts such as SAGE (Fazey et al., 2014). It also allows local institutions to carry forward data analysis and integration beyond the life of a single research project.

When stakeholders are involved in research design and data collection, the resulting outputs are more readily understood and trusted, leading to faster and more effective application in the field (Cvitanovic et al., 2016). This helps close the gap between scientific research and real-world management—especially important in dynamic environments like riparian zones, where ecological processes and human pressures intersect.

Well-structured, co-produced datasets create the baseline for evidence-based adaptive management. In riparian systems, this means being able to spatially prioritize restoration zones, track vegetation recovery, and assess the effectiveness of buffer widths and ecological connectivity (Capon et al., 2013; Seavy et al., 2009). By integrating ecological monitoring with policy tools (e.g., SDAGE, Nature Restoration Regulation), data production supports iterative learning cycles and more resilient ecosystem governance.

## 5.5. Context

This study forms part of a broader cluster of interdisciplinary internships coordinated under the SAGE *Loire en Rhône-Alpes* initiative. This collective project aims to develop consistent and scalable methods for characterizing and monitoring riparian vegetation in the study area. The *Loire* department's riparian zones are currently assessed using fragmented and inconsistent indicators, often applied only to subsets of the territory. This fragmented data landscape—comprised of disparate land-use maps, vegetation inventories, and localized hydrological indices—limits the capacity for cohesive management or cross-regional comparison. Existing tools like the IBC-R index or the emerging Ripascan protocol remain inconsistently deployed, further complicating efforts to synthesize ecological status assessments across the catchment.

In response, this internship contributes to the design and implementation of a spatially explicit methodology for mapping riparian zones across the entire study area. It emphasizes a harmonized and replicable approach that can integrate ecological, geomorphological, and land-use variables.

Within the internship cluster, complementary efforts address related challenges—ranging from evaluating forest ecological function and biodiversity to modeling riparian impacts on water temperature and flow dynamics. Together, these parallel studies support the development or the validation of robust and multi-scalar indicators.

## 5.6. Data Availability

The spatial analysis conducted in this study relied on a variety of openly accessible and high-resolution geospatial datasets provided by national and institutional sources. The foundational topographic and hydrographic layers, including stream networks and land cover features, were sourced from the **BD TOPO** and **OCSGE** databases published by the French National Institute of Geographic and Forest Information (**IGN**). High-resolution LiDAR data (classified point clouds at 1 m resolution) were also made publicly available by IGN as part of the **LiDAR HD** campaign and proved critical for detailed vegetation structure extraction. Aerial orthophotos were obtained from **BD ORTHO**, supporting both vegetation validation and land use classification. The availability of such high-quality national datasets significantly enhances the reproducibility, scalability, and operational utility of geomatics-based riparian studies in France.

## 5.7. Problem Statement

How can riparian vegetation extent, continuity, and structural attributes be effectively characterized across large watersheds using integrated geomatics approaches—particularly GIS and airborne LiDAR—to support ecological restoration and conservation under climate change and anthropogenic pressures?

### 5.7.1. Objectives

- Develop a robust, replicable method for mapping riparian vegetation across the Loire en Rhône-Alpes watershed.
- Generate spatial indicators of riparian structure, extent, and connectivity to inform ecological status assessment.
- Create reference layers to support practitioners, researchers, and decision-makers in restoration planning and monitoring.

### 5.7.2. Hypotheses

- Combining high-resolution LiDAR and GIS analysis provides more accurate and actionable riparian vegetation mapping than conventional vector data alone.
- Riparian vegetation structure and connectivity are strongly correlated with valley bottom morphology and proximity to hydrological networks.
- Integrating geomatics-based indicators can highlight spatial priorities for restoration by identifying fragmented or degraded riparian zones across the SAGE.



## 6. Study Area

The SAGE *Loire en Rhône-Alpes* study area is situated within France's *Massif Central*, characterized by a complex assemblage of crystalline and metamorphic rocks, including granites, gneiss, and schists originating from the Paleozoic era (Quenardel et al., 1991) (Figure 2). These formations give rise to several prominent mountain ranges: the *Monts du Forez*, *Bois Noirs*, and *Monts de la Madeleine* to the west, and the *Monts du Lyonnais* and *Monts du Beaujolais* to the east. To the southeast lies the granitic *Pilat* Massif, noted for its geological diversity and varied landscapes (Faure et al., 2005).

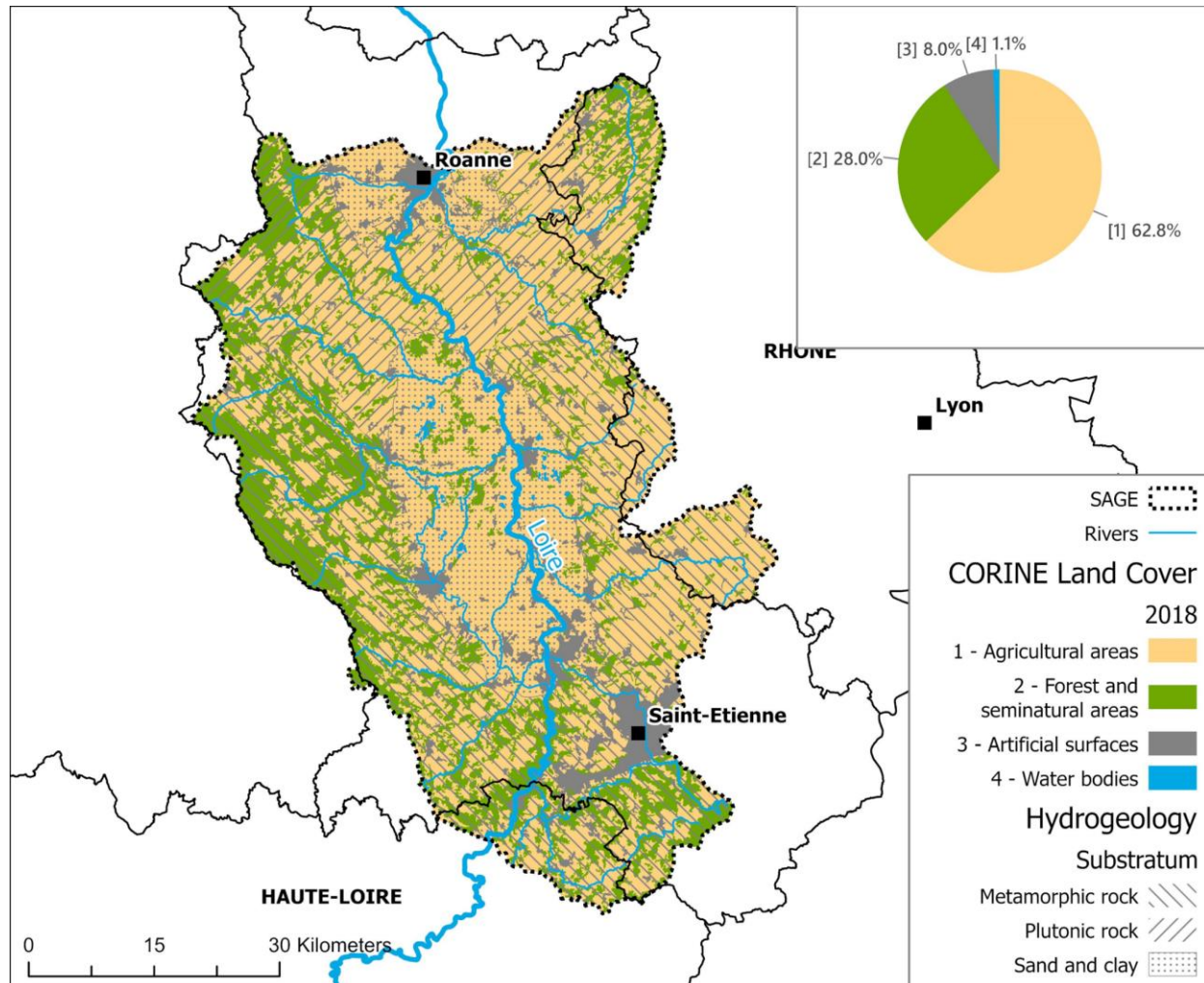


Figure 2: Land cover and geology of the SAGE Loire en Rhône-Alpes. Sources: CORINE LAND COVER, BRGM

The region is also comprised of sedimentary basins such as the *Forez* and *Roannais* plains, primarily composed of Tertiary and Quaternary sediments (Vitel, 2001). These plains are separated by the historically significant *Stéphanoise* depression, a coal basin that played a pivotal role in the area's industrial development (Boudrie, 2004).

Topographically, the study area exhibits marked contrasts spanning around 4000 km<sup>2</sup> (SAGE LRA, 2014). The western mountain ranges, *Monts du Forez*, feature rugged terrain, steep slopes, deep valleys, and high peaks, reaching an elevation of 1,634 meters, making it the highest point in this

range(SAGE LRA, 2014). These uplands are often cloaked in dense forests, peatlands and display sharp altitudinal gradients going downstream. In contrast, the *Forez* and *Roannais* plains present relatively flat landscapes, generally ranging between 300 and 500 meters in elevation, facilitating extensive agricultural activities and significant urban development. The eastern and southeastern areas, including the *Monts du Lyonnais*, *Monts du Beaujolais*, and *Pilat* Massif, offer more moderate altitudes, typically below 1,000 meters, characterized by rolling plateaus, gentle slopes, and narrow valleys, contributing to distinct local microclimates (Faure et al., 2005; SAGE LRA, 2014).

Climatically, the SAGE Loire en Rhône-Alpes region experiences a temperate regime with pronounced seasonal variations. Winters and autumns typically bring higher water levels and significant precipitation, whereas summers are notably drier, imposing considerable hydrological stress on local aquatic ecosystems. Climate projections indicate significant changes, with temperature increases between +3°C to +6°C anticipated by the end of the century. Winter precipitation is expected to rise by approximately 20%, while summer rainfall may decrease by up to 30%, leading to prolonged drought conditions and a heightened frequency of intense rainfall events (EPTB Loire, n.d.)

Land use in this region predominantly revolves around agriculture, occupying about 50% of the total territory (SAGE LRA, 2014). Agricultural land is largely dedicated to livestock farming, especially dairy production and forage cultivation. Intensive cereal production is also significant, particularly within the *Forez* Plain (SAGE LRA, 2014).

The territory comprises approximately 290 communes and hosts two major urban centers: *Saint-Étienne*, totaling 677,538 with around 175,318 inhabitants, and *Roanne*, with approximately 35,750 inhabitants in 2007 (SAGE LRA, 2014). Historically, this region has been an industrial hub, particularly along the *Ondaine/Saint-Étienne/Gier* corridor. Dominant industrial sectors include metalworking, textiles, plastics, and wood industries.

Hydrologically, the Loire River serves as the primary watercourse of the region, alternating between deep, narrow gorges and extensive sedimentary plains. Key hydraulic infrastructures include the *Grangent* and *Villarest* dams, instrumental in regional water management strategies, flood control, and drought mitigation (EPTB Loire, n.d.; Galtier & Guillaume, 2004). Several small and bigger canals cross waterways along the whole sage extent, those being dedicated mostly to irrigation during dryer months.

## 7. Material and methods

This will present the methods used during this internship. Please note that during almost the whole length of the internship, a part of the north west corner of the study area was missing LiDAR data, which became available during the writing of this report, so the DEM was created from this data, but none of the metrics were re-calculated. Please note as well that generative AI was used in order to fine-tune the R and python scripts.

### 7.1. Valley bottom

The delineation of valley bottoms represents a foundational step in riparian vegetation analysis, as it spatially defines the domain within which riparian processes, structures, and

vegetation communities are most likely to develop. Valley bottoms are the product of long-term fluvial and geomorphological processes and are commonly defined as the low-lying areas adjacent to streams and rivers that are subject to frequent hydrological influence, sediment deposition, and lateral channel movement (Piégay et al., 2005; Stella et al., 2013). In ecological terms, these areas host some of the most dynamic and biologically diverse habitats due to their periodic connectivity with the watercourse and the presence of fertile alluvial soils (Capon et al., 2013; Naiman et al., 1993).

The purpose of delineating valley bottoms in this study was to constrain the spatial analysis of riparian vegetation to hydro-geomorphologically relevant zones. This is particularly important in the study area, where a strong topographic gradient results in narrow, steep-sided valleys in upland areas and wider, low-slope alluvial plains downstream. Without an objective valley bottom

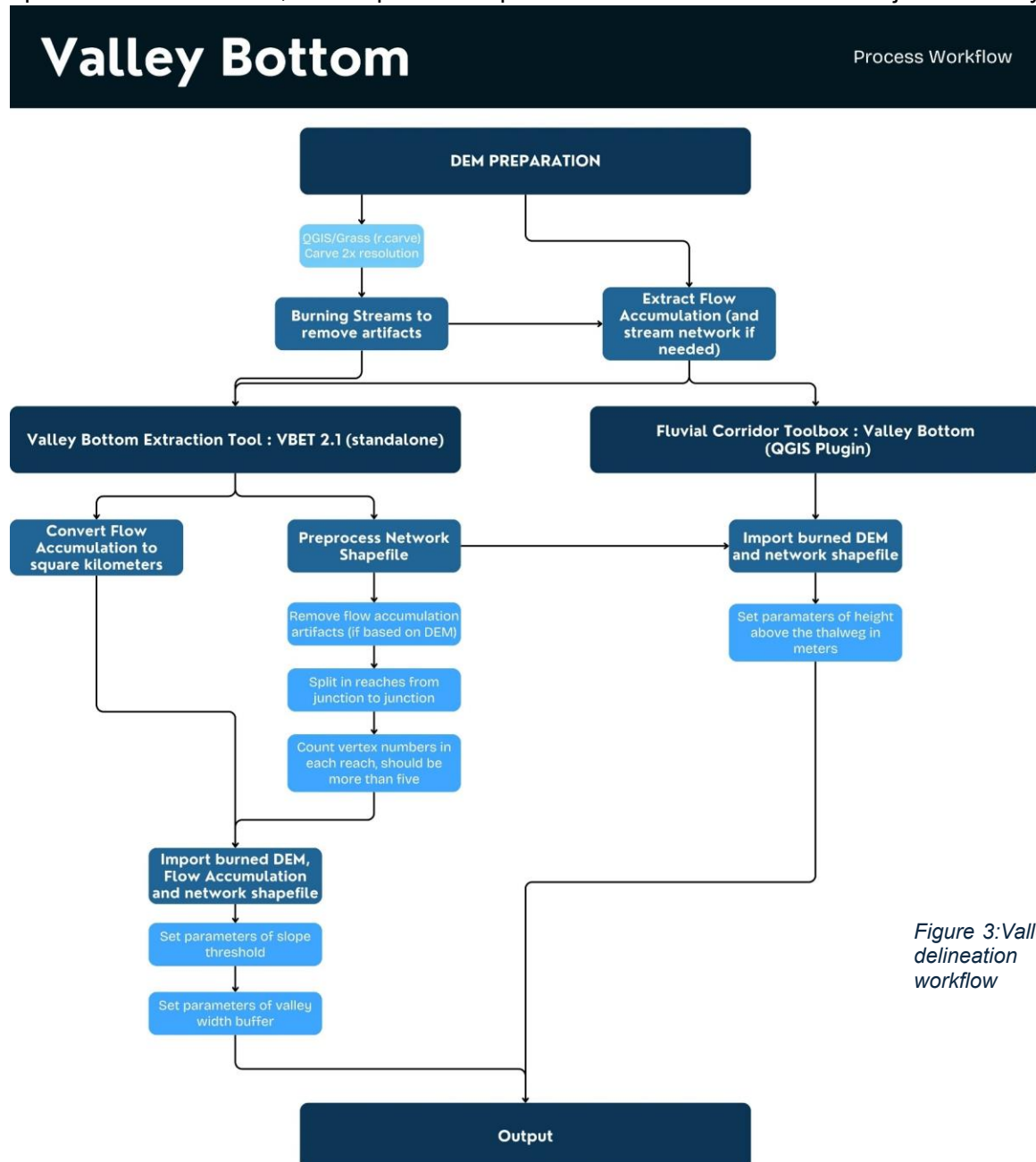


Figure 3: Valley bottom delineation process workflow



boundary, riparian vegetation might be falsely interpreted outside of its functional zone, thus biasing ecological and structural assessments.

For this study, high-resolution digital elevation data derived from LiDAR HD (5-meter resolution) (R script in Appendix 5), made available by the IGN, was used as the base dataset. Initially, the RGE ALTI DEM was used but due to many incoherences (Appendix 1), primarily caused by the aggregation of data (Appendix 2). The resultant DEM of difference (Appendix 3) between the RGE ALTI DEM and LiDAR HD DEM prove major differences that can have an impact on the valley bottom result.

Prior to analysis, the stream network was cleaned of all the canals (small and large) due to output incoherences. Canals creates large polygons output, because of the intersecting of lines in two different points, making the algorithm “think” that it is one really large river (in the first tests, the polygons were covering half of the sage area).

The digital elevation model was hydrologically corrected using tools available in the GRASS GIS software suite using the “r.carve” modules. This tool ensure topographic continuity in the drainage network by removing artificial barriers such as roads or bridges that may otherwise disrupt the modeled flow path (Soille et al., 2003). The “r.carve” function was particularly useful for maintaining hydrological realism along valley floors in urban or infrastructure-dense areas. The carve width used was two time the resolution (here 10 meters).

Two valley bottom delineation tools were initially compared: the Fluvial Corridor Toolbox (FCT) and the Valley Bottom Extraction Tool (VBET) (Figure 3). The FCT, a QGIS plugin developed to simplify geomorphic corridor mapping, operates by applying a uniform vertical buffer above the channel elevation to define the lateral extent of the valley floor (Clubb et al., 2017). Although straightforward to implement, this approach has several drawbacks, including a reliance on user-defined Z thresholds and limited responsiveness to changes in valley morphology or hydrological conditions.

The VBET, developed by the Utah State Univeristy, was ultimately selected due to its multi-criteria, spatially adaptive, and fully automated approach (Figure 4). VBET uses a combination of DEM-derived slope metrics, flow accumulation surfaces, bankfull channel height estimates, and confinement thresholds to delineate valley bottoms across large river networks. It begins by

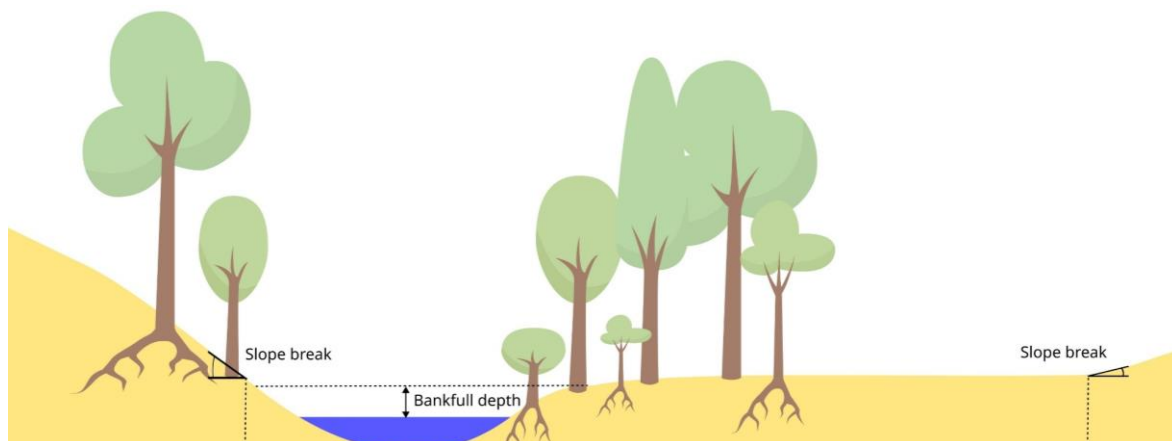


*Figure 4: Input and output parameters of the valley bottom extraction tool on a cross section of a theoretical river and associated floodplain.*

detrending the DEM relative to the longitudinal profile of the stream, which allows the tool to evaluate topographic relationships perpendicular to the flow direction. Flow accumulation thresholds are then applied to identify major and minor drainage features. Slope breaks and changes in channel confinement are used to define the lateral boundaries of the valley bottom. Empirically or literature-derived estimates of bankfull width and height help refine the corridor boundary, making the output context-sensitive to stream size and valley geometry (Gilbert et al., 2016).

The output of VBET is a continuous polygon layer representing the valley bottom along the streams of the study area. This layer was subsequently used as a mask for all vegetation extraction and continuity assessments, ensuring that only those vegetation features with a likely hydrological connection to the fluvial system were retained. The accuracy of the delineated valley bottoms were cross-validated using Q100 flood extents from regional hydrological modeling data, as well as a web-map available for practitioners.

## 7.2. Vegetation delineation

Accurate delineation of riparian vegetation is essential for assessing the structure, extent, and continuity of riparian corridors. These vegetative zones play critical ecological roles in water quality regulation, habitat provision, bank stabilization, and microclimate moderation (Naiman et al., 1993; Riis et al., 2020). However, due to their narrowness, spatial heterogeneity, and dependence on fine-scale topographic and hydrological gradients, riparian zones are difficult to map precisely using conventional cartographic datasets or medium-resolution remote sensing imagery (Macfarlane et al., 2017; Michez et al., 2017).

Initial attempts to characterize vegetation relied on the French national land cover dataset “*Zone de Végétation*” provided by the IGN. While informative at larger scales (1:25,000), this vector dataset lacks precision to look at a narrow corridor around a river, and uses a minimum mapping unit of 5,000 m<sup>2</sup> and represents smaller features as generalized hedgerows or mixed-use patches. This granularity proved insufficient for delineating riparian bands or isolated trees common along headwaters and cultivated valleys. Although a major update occurred in 2015, parts of the dataset still reflect field data from 2009, resulting in temporal mismatch with the current state of vegetation. These limitations were evident during field comparisons, where significant discrepancies were observed between mapped polygons and actual vegetated zones—especially along small watercourses and recently reforested riparian segments.

To overcome these challenges, this study adopted a LiDAR-based vegetation extraction method using the national LiDAR HD dataset released by IGN in 2022. The approach focuses on extracting vegetation structure directly from the classified point cloud, rather than relying on multispectral indices or historical vector layers. Specifically, vegetation was delineated by isolating all LiDAR points classified as “high vegetation” (class 5)—corresponding to vertical structures such as shrubs and trees—within a vertical threshold of at least 2 meters above ground.

### Vegetation coverage differences between database and in situ observations

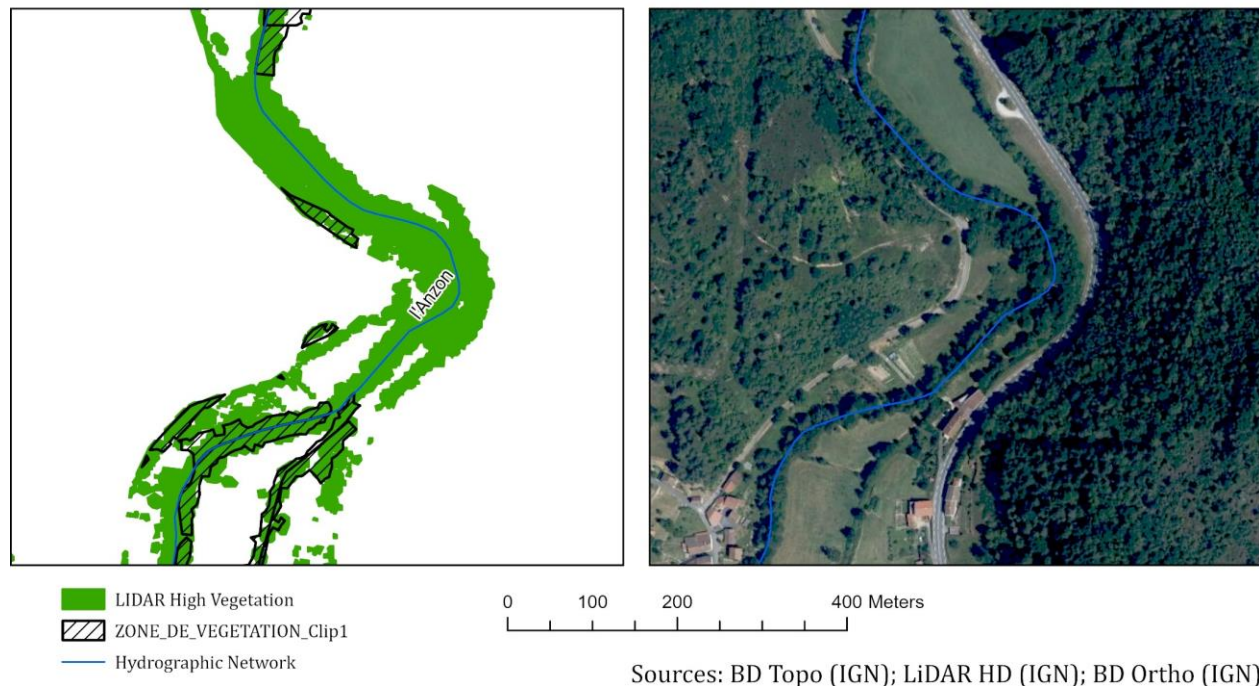


Figure 5: Differences between the IGN vector layer and the extracted vegetation layer from the classified LiDAR, with visual comparison

These points were then vectorized using a density-based clustering algorithm, generating a new polygon layer representing continuous patches of high vegetation. This delineation allows for a sub-meter precision in identifying riparian forests, accounting for both dense forest blocks and fragmented vegetated areas. Moreover, the use of classified LiDAR returns improves resilience against errors introduced by shadowing or canopy cover, common issues in optical remote sensing (Michez et al., 2017; Stackhouse et al., 2023).

The method was implemented using a tool in QGIS, the point cloud boundary tool. The outputs were validated visually against high-resolution aerial orthophotos (BD Ortho IGN, 2022) and via field verification along segments of the *Lignon* and *Anzon* rivers, with the help of QField maps.

One of the major outcomes of this LiDAR-based approach was the clear demonstration of its superiority over IGN vector vegetation data, particularly in confined valleys or recently afforested banks. As shown in the comparative analysis (Figure 5), large mismatches occurred where small riparian forests were not represented in the IGN dataset but were clearly identified in the LiDAR data. These mismatches were particularly prominent in agricultural areas and around infrastructure, where thin riparian bands are most likely to be excluded in coarse-resolution products.

### 7.3. Longitudinal continuity

The methodological approach was designed as a rapid diagnostic tool to support the selection of relevant sampling and validation sites for subsequent detailed analyses. It involved identifying the presence or absence of high vegetation cover adjacent to streamlines and hydrographic polygons using airborne LiDAR and cartographic data.

First, a geometry representing the two banks of the fluvial corridor was constructed. Two data sources were used: the OCSGE polygon layer, specifically the "water surfaces" class, and the BD TOPO line layer representing hydrographic stream networks. From the BD TOPO stream lines, two lateral buffer lines were generated on each side of the stream using a fixed offset. These buffers approximate potential riparian corridors on both banks, especially where polygonal water representations were absent or fragmented.

The resulting geometries (OCSGE water surfaces and lateral buffers from BD TOPO) were merged to form a continuous candidate layer for riparian presence assessment. This unified layer was then spatially intersected with the LiDAR-derived high vegetation layer, which had previously been extracted using classified point clouds (vegetation class 5) and vectorized into polygonal features. Each segment of the fluvial corridor was then classified based on whether it intersected this vegetation layer, distinguishing vegetated from non-vegetated streambanks.

To reduce noise and account for minor classification gaps due to LiDAR occlusions or processing artifacts, a refinement was applied. Any non-vegetated line segments smaller than 10 meters in length, and entirely surrounded by vegetated segments, were reclassified as vegetated. This post-processing step aimed to better reflect field-observable continuity and mitigate artificial breaks in continuity caused by data resolution or vegetation segmentation errors.

Ultimately, the analysis yielded a binary longitudinal continuity classification (vegetated vs. non-vegetated) along the linear hydrographic network. While preliminary in nature, this method provided essential spatial information for identifying zones with strong or weak vegetation continuity, facilitating field validation and helping define areas for more detailed buffer-based riparian assessments.

### 7.4. Vegetation Density

Vegetation density, particularly in riparian zones, serves as a critical indicator of ecosystem health, structural complexity, and potential ecological functionality (Naiman et al., 1993; Riis et al., 2020). The estimation vegetation density was essential to differentiate riparian areas by their degree of coverage and canopy complexity, which are closely linked to their role in filtering nutrients, stabilizing banks, and offering habitat continuity.

This metric was computed using the lidR package in R (Roussel et al., 2020), which allows the fast computing of large datasets. A variable window function, defined as  $0.003 \times \text{point height} + 4$  meters, was used to account for the variation in tree size and canopy width, improving crown delineation accuracy in heterogeneously structured forests. This dynamic approach was adapted from boreal forest studies but was applied here cautiously, acknowledging the structural differences in temperate deciduous riparian systems.

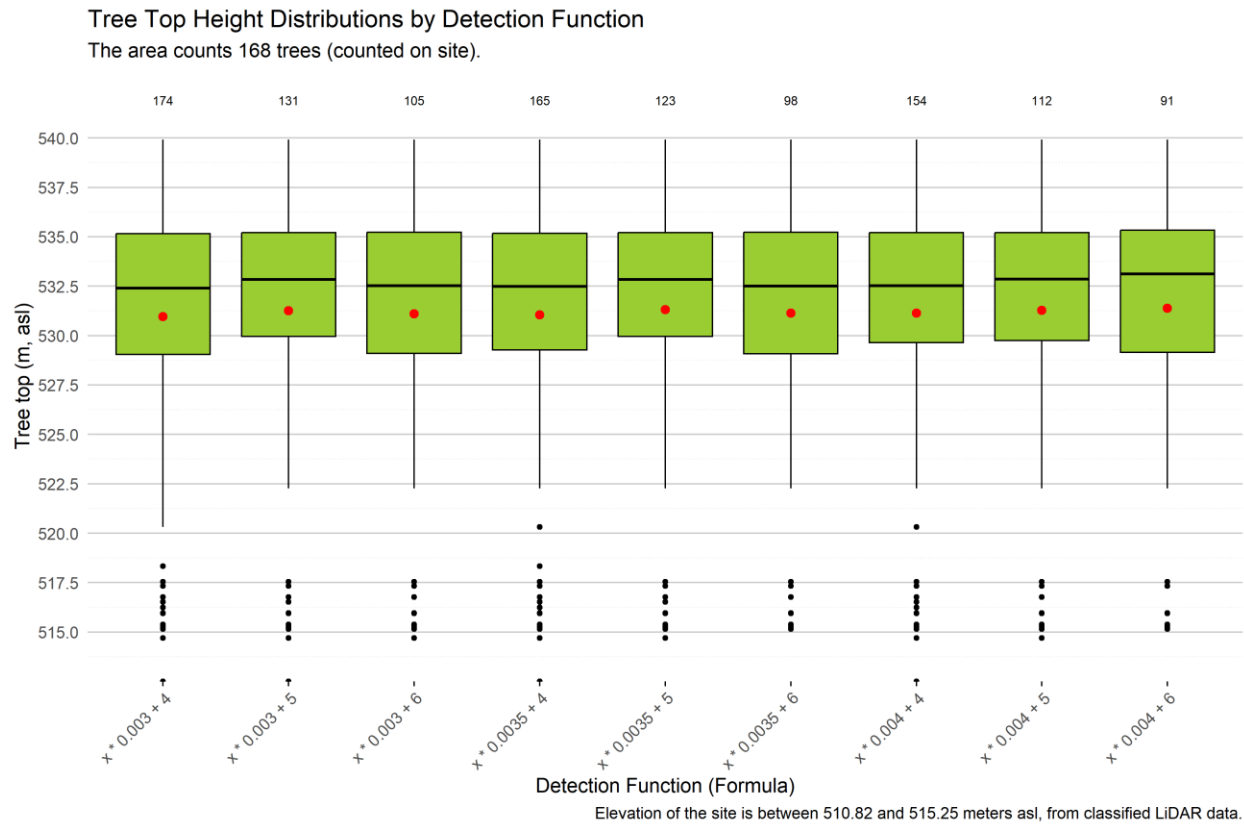


Figure 6: Formula calibration for the algorithm. Numbers on top of the boxplot are the number of trees detected.

Validation of the vegetation density outputs was performed through two methods. First, visual verification was conducted using field data collected around vegetated places in Saint-Étienne, comparing the LiDAR-extracted vegetation patches to actual tree positions identified on site (Appendix 4a and 4b). Second, a cross-comparison with high-resolution aerial imagery (BD ORTHO, IGN) was made to ensure general consistency between high vegetation zones and optical signatures of canopy cover. While the approach yielded robust density patterns in forested headwaters and broad alluvial valleys, it underperformed in narrow riparian strips and urban-adjacent areas, where LiDAR point occlusion and lower return densities introduced spatial noise.

Then field validation were made on one of the ecology internship study sites, where approximately 25x25 meters quadrats were defined and trees were counted inside. The three quadrats represents three different types of species repartition, according to management efforts made on this river: number one untouched, mixed species (*Alnus glutinosa*, *Fraxinus excelsior*, *Salix alba*, *Robinia pseudoacacia*), number two, fully restored (*Alnus glutinosa*, *Fraxinus excelsior*, *Salix alba*, *Populus nigra*), and the third one, only invasive species (*Robinia pseudoacacia*).

However, the method lies in its inability to fully capture understory vegetation and low shrub cover, which are often essential components of riparian structure but are masked under dense canopies or filtered out by classification thresholds. Additionally, segmentation of individual tree crowns—necessary for estimating biomass or functional metrics—was not reliably achieved using the tree detection function in lidR, due to its original design for coniferous canopies in North America (Roussel et al., 2020). While alternatives such as the lidRtrees plugin developed by INRAE offer



improved segmentation using CHM-based analysis, these methods are computationally intensive and require careful pre-processing of digital terrain and canopy models (Monnet, 2010; Pitkänen et al., 2001; Popescu & Wynne, 2004).

The final point vector file provides also the elevation above sea level of the tree top, on which can be subtracted the DEM elevation to obtain a tree height for each detected tree.

## 7.5. Lateral Continuity

Lateral continuity refers to the presence and structural coherence of riparian vegetation across multiple distances perpendicular to the stream channel. This aspect of riparian connectivity is essential for buffering hydrological and ecological interactions between aquatic and terrestrial systems, including flood attenuation, sediment trapping, nutrient retention, and wildlife habitat provision (Naiman et al., 1993; Riis et al., 2020). In fragmented landscapes or areas under anthropogenic pressure, the lateral spread of vegetation is often constrained by agriculture, urban development, or infrastructure, leading to weakened riparian functionality (Capon et al., 2013; Dufour et al., 2019).

In this study, lateral continuity was assessed using a multi-buffer zonation approach applied to all stream reaches in the SAGE Loire en Rhône-Alpes area. Three concentric buffer zones were

### Creation of buffers

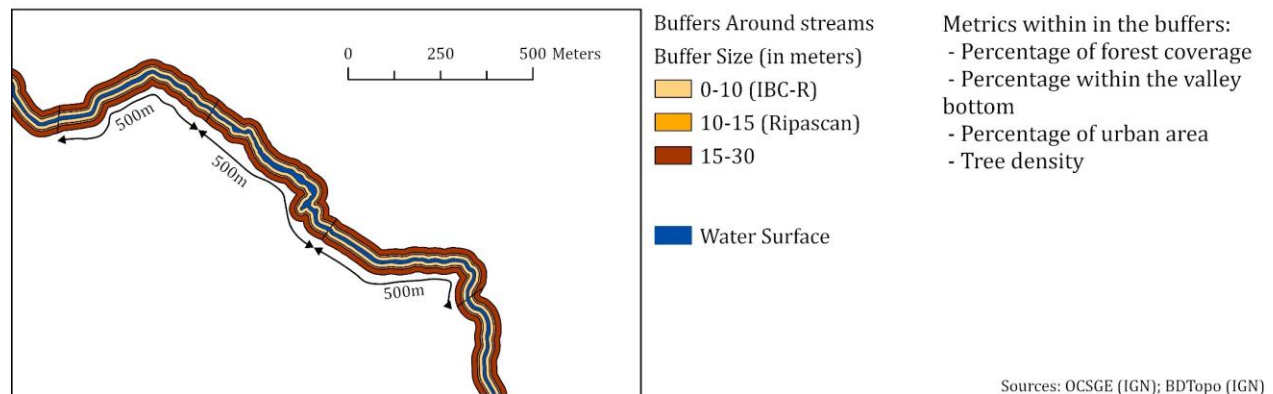


Figure 7: Creation of 500m long riparian buffers along streams.

generated on both sides of each stream: the first at 10 meters, the second at 15 meters, and the third at 30 meters from the stream centerline. These distances were selected based on both ecological rationale and compatibility with established indices such as the French IBC-R (Janssen et al., 2021) and the Ripascan method (Staentzel, 2025), which recommend minimum buffer widths of respectively 10 and 15 meters for riparian quality assessment. The 0-10 and 10-15 meter buffers captures the immediate riparian strip, often considered the ecologically most sensitive zone, while the 15-30 meter extent provides an overview of broader landscape interactions.

Each buffer zone was analyzed for key land cover variables: the proportion of high vegetation (extracted from classified LiDAR data), the percentage of impervious or artificialized surface (from the OCSGE database), and the presence of agricultural land. Using spatial overlay analysis in

ArcGIS Pro and QGIS, these variables were intersected with the buffer polygons and their relative proportions calculated for each 500-meter reach segment.

## 7.6. Evaluation Matrix

The evaluation matrix method is a key component of this study's approach to classifying riparian forest quality along the river network of the study area. Designed to translate high-resolution spatial data into actionable ecological insights, this methodology synthesizes the condition of riparian vegetation at the standardized 500-meter stream reach scale. It does so by aggregating qualitative assessments derived from multi-distance buffer zones into a composite score that reflects the potential ecological functionality and structural integrity of riparian zones.

The initial phase of the method relies on the previously created buffer zones. These zones reflect varying degrees of influence from the watercourse, with the innermost buffer capturing immediate riparian vegetation and the outermost representing transition areas influenced by surrounding land use. Each buffer is spatially tagged with an identifier (ID\_BUFF) representing its proximity rank (from 1 to 3) and is analyzed for three key attributes: proportion of high vegetation, impervious surface cover (derived from OCSGE), and the vegetation density metric derived from LiDAR data.

Each buffer's condition is translated into a qualitative score—ranging from “Very Good” to “Bad”—based on thresholds established through a combination of literature benchmarks and field observation. These qualitative classes are then assigned numerical values from 5 (Very Good) to 1 (Bad), while zones dominated by urban cover or non-riparian features are excluded from the scoring process. This translation provides a standardized and quantitative means of aggregating ecological information across multiple scales of analysis (Breton et al., 2023). The reasoning was based on the Spanish QBR index (Segura-Méndez et al., 2023), even though all the data were not the same, it provided a track to follow.

The second phase involves consolidating buffer scores into a single evaluation for each river reach. This is accomplished through a weighted averaging system, where each buffer's contribution is adjusted based on its importance. Inner buffers are weighted more heavily than outer ones, reflecting their stronger ecological significance and direct connection to aquatic habitats. The formula applied is a classical weighted average:

$$\text{Weighted Score} = (\sum \text{Score} \times \text{Weight}) / (\sum \text{Weight})$$

Only buffers with valid scores are considered in the computation, and any missing or invalid data (e.g., due to urban masking or classification error) are excluded from the calculation to maintain consistency and data integrity.

Once the weighted average score is calculated for each 500-meter segment, it is reclassified into a final qualitative class. The classification scheme follows clearly defined thresholds: a score  $\geq 4.5$  is classified as “Very Good,” 3.5 to  $< 4.5$  as “Good,” 2.5 to  $< 3.5$  as “Moderate,” 1.5 to  $< 2.5$  as “Poor,” and  $< 1.5$  as “Bad.” This final classification is appended to the line dataset representing the river network, thus enabling visualization, spatial analysis, and prioritization of restoration or conservation actions at a management-relevant scale.

To operate this process, a custom Python-based script tool was developed within ArcGIS Pro. This tool automates the workflow, from buffer-score extraction to reach-level aggregation and classification. It ensures that the process is replicable, scalable, and resilient to variations in dataset completeness or quality. This tool supports iterative use, allowing updates to be made as new LiDAR acquisitions or land cover datasets become available, enhancing the long-term utility of the method in dynamic landscapes.



## 8. Results

### 8.1. Valley Bottom Delineation

#### Valley bottom delineation

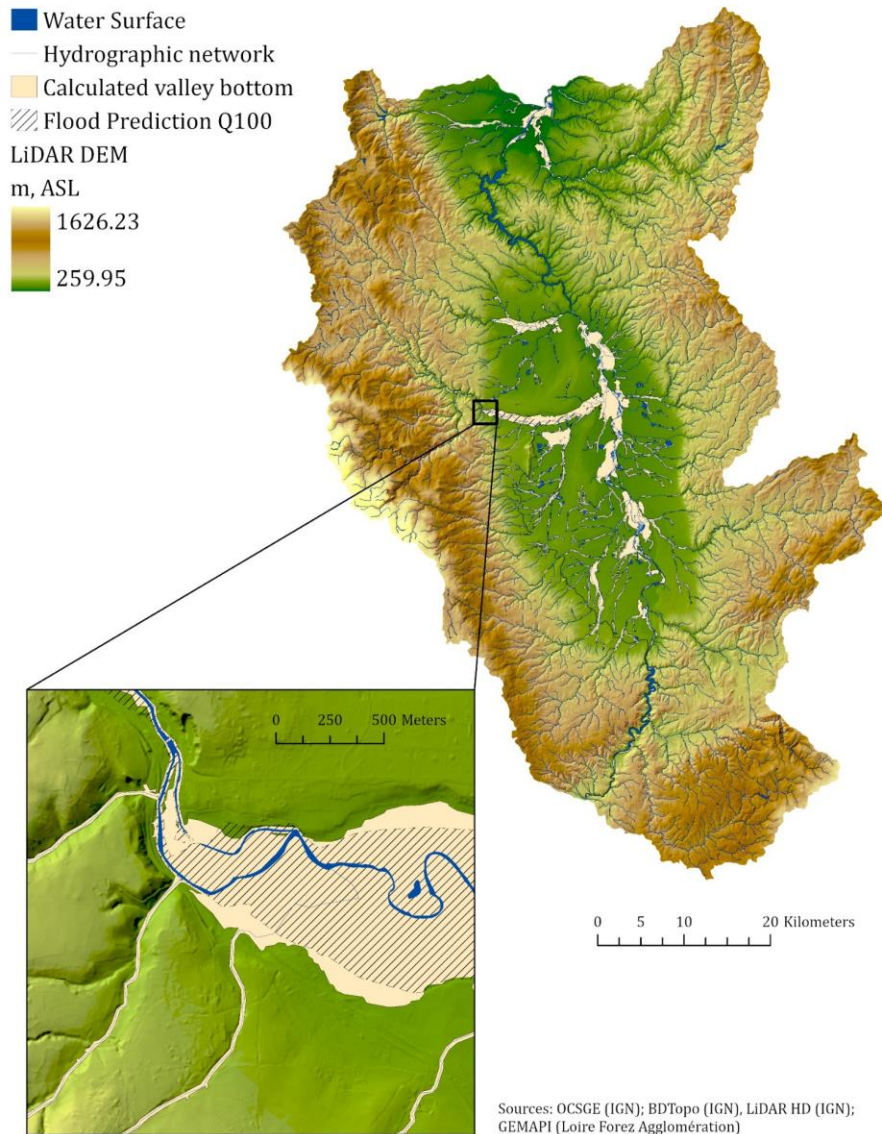


*Figure 8: Result of the valley bottom delineation, with a zoom on Boen sur Lignon, and compared with the Q100 flood prediction from Loire Forez Agglomération, in charge of this watershed.*

This result illustrates the delineation of the valley bottom using the Valley Bottom Extraction Tool (VBET) applied to a pre-processed digital elevation model (DEM). The carved DEM ensured uninterrupted hydrological flow by eliminating artificial barriers such as roads or infrastructure. The output highlights low-lying alluvial zones that could potentially host riparian vegetation, with a spatial extent that reflects topographic confinement. This layer served as a fundamental spatial boundary for further vegetation analysis, delimiting the ecological potential of riparian corridors across the watershed.

## 8.2. Vegetation Delineation

### LiDAR Vegetation Extraction

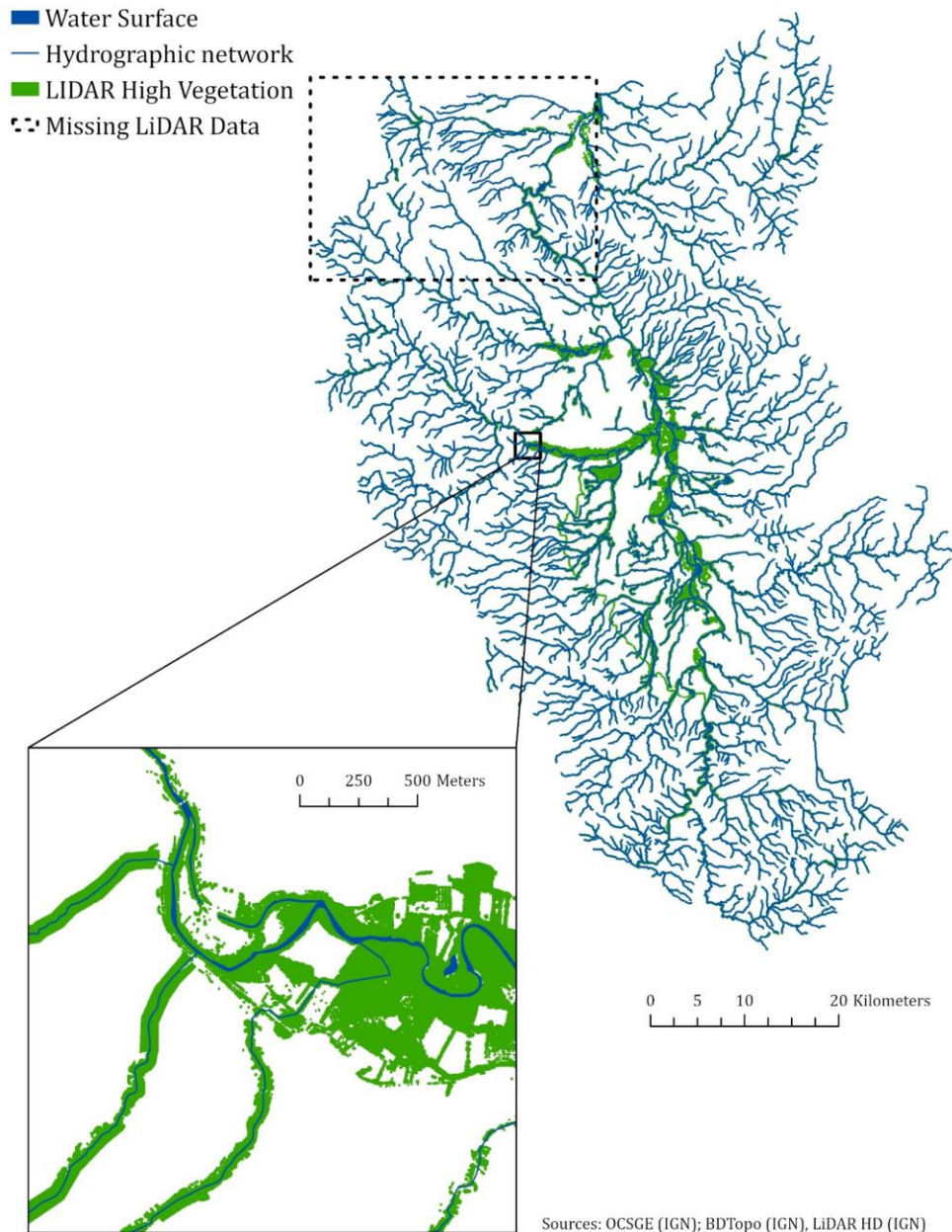


Figure 9: Result of the forest delineation from LiDAR, with a zoom on Boen sur Lignon.

High vegetation was extracted from classified LiDAR data using class 5 points, corresponding to tall woody vegetation. The result provides a detailed spatial footprint of tree cover, extending beyond standard forest polygons available in existing datasets. This fine-resolution delineation enabled detection of small or fragmented riparian woodlands, offering an accurate vegetation mask for later overlay analyses. It highlighted discrepancies with IGN forest layers and demonstrated the method's ability to detect isolated trees or narrow strips of riparian cover otherwise omitted in vector-based sources.

### 8.3. Longitudinal Continuity

## Longitudinal Continuity Analysis

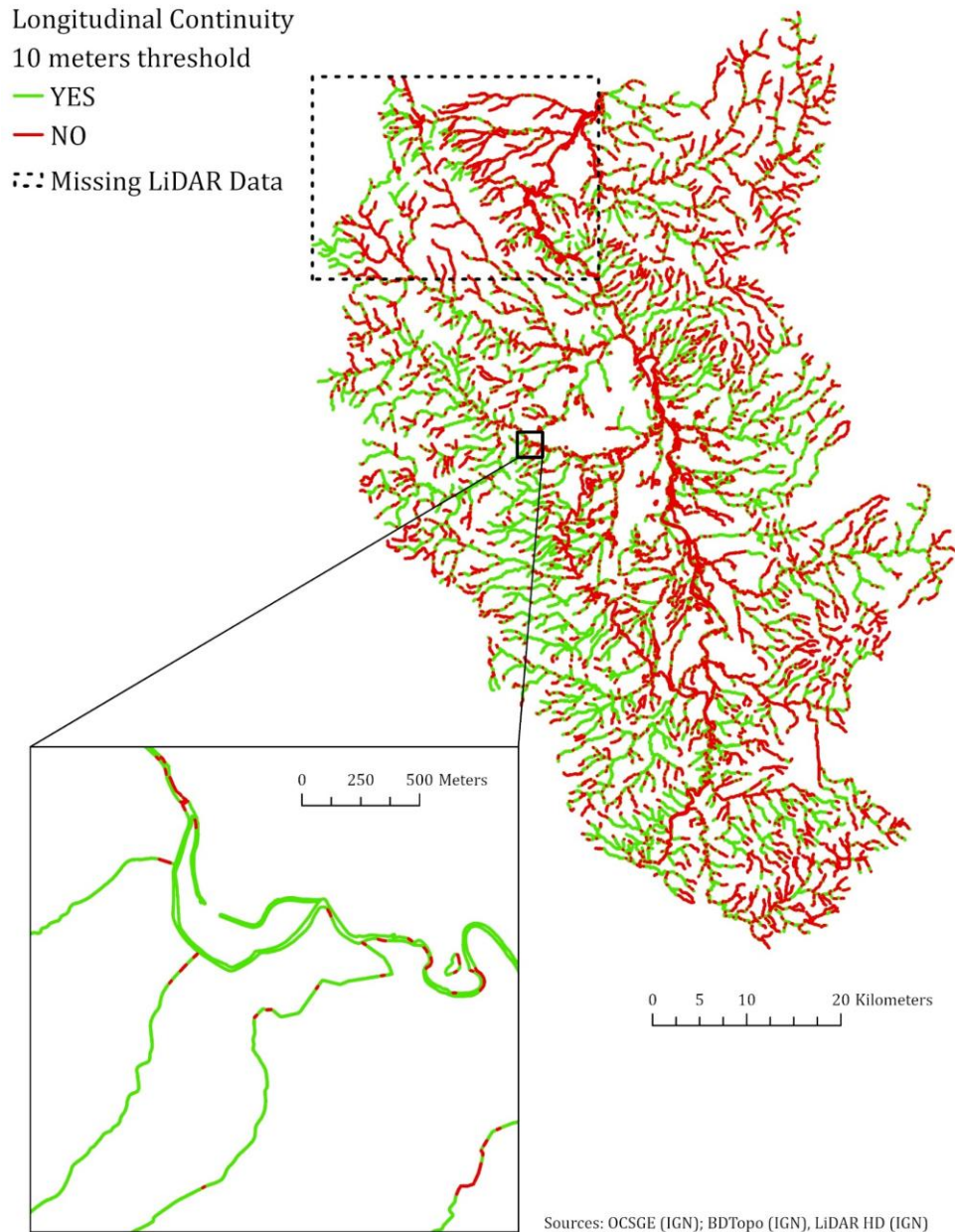


Figure 10: Result of the longitudinal continuity analysis, with a zoom on Boen sur Lignon.

This result shows the presence or absence of high vegetation along the stream network, visualized through segmented lines derived from hydrographic data. Sections touching the LiDAR vegetation polygons were labeled as vegetated, while gaps were flagged as discontinuities. This binary classification enables an evaluation of longitudinal ecological continuity, essential for identifying fragmentation points and planning restoration efforts. Notably, small gaps (<10 m) surrounded by vegetated segments were smoothed to reduce false positives caused by data noise.



## 8.4. Vegetation Density

### Tree Density on La Bathie d'Urfé (Lignon)



Figure 11: Result of the density analysis by applying the tree top method, with the represented quadrats counted on site, representing three different typologies of forest.

Sources: BDTopo (IGN), LiDAR HD (IGN), BD Ortho (IGN)

This result presents the estimation of tree density within the riparian zone near *La Bathie d'Urfé* along the *Lignon* River. Individual trees were extracted from the LiDAR. The delineated high vegetation area (in green) corresponds to LiDAR class 5, indicating significant canopy cover. Overlaid on this layer are three yellow field validation quadrats used to compare remote-sensed estimations with in-situ observations. The map demonstrates the feasibility of extracting tree-level data at fine scales and its relevance for estimating structural complexity. However, segmentation of individual trees proved challenging in dense forest patches, especially where canopy overlap is high—an expected limitation when applying crown detection methods developed primarily for boreal coniferous systems, underestimating the number of tree by a factor 4.3, constant on the three sampled places.

## 8.5. Lateral Continuity

### Lateral Continuity Analysis

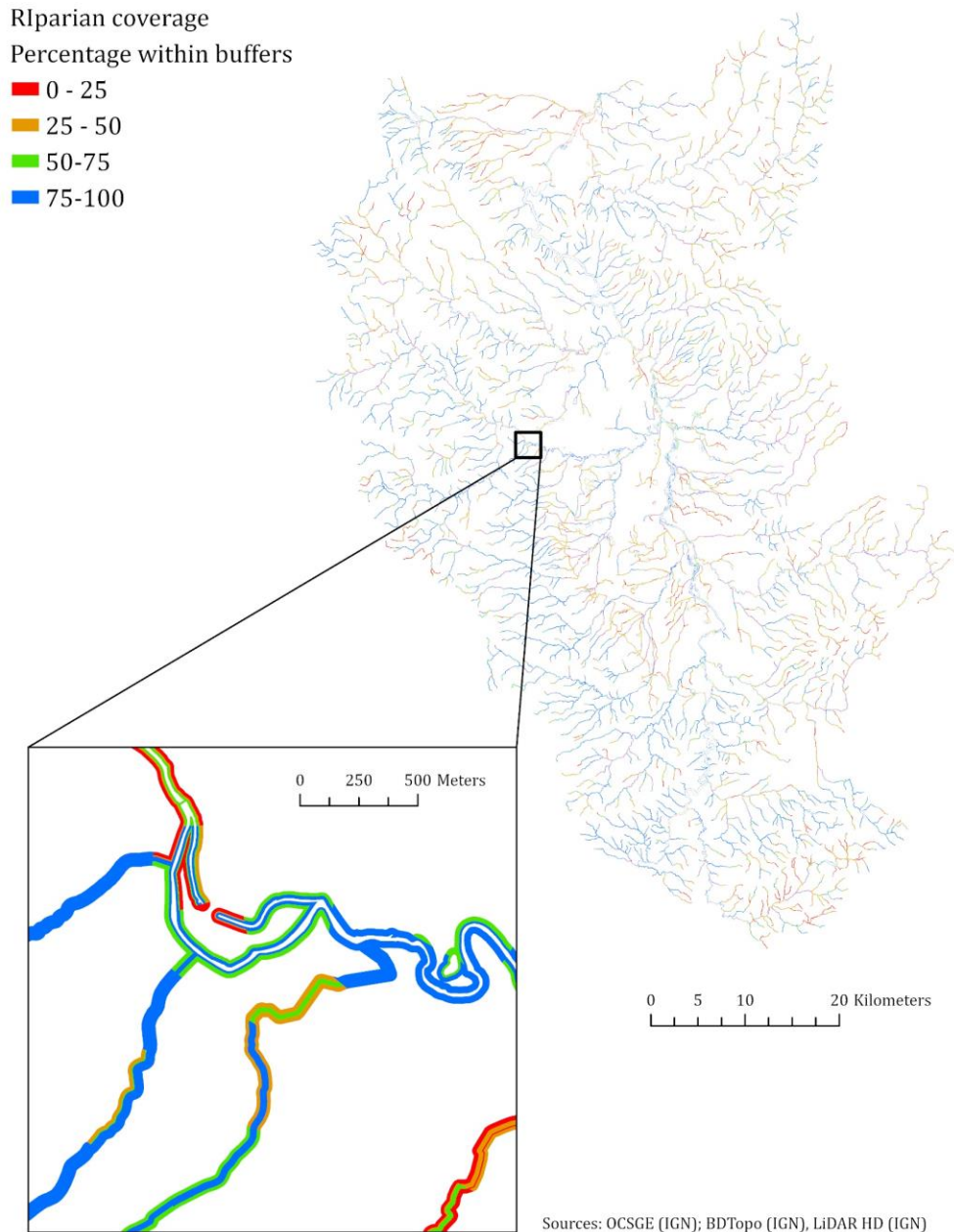


*Figure 12: Result of the lateral continuity analysis, here representing the percentage of coverage of buffers by forest, with a zoom on Boen sur Lignon.*

Lateral continuity was assessed using nested buffers (10 m, 15 m, 30 m) along the stream network. This result shows how much of each buffer zone overlaps with high vegetation and valley bottom areas. The visual output illustrates areas where vegetation remains confined to narrow riparian strips or extends more broadly into floodplains. By summarizing this information per 500 m stream reach, this approach allows integration into existing ecological indices, such as the IBC-R and Ripascan, and facilitates spatial comparisons across the SAGE territory.

## 8.6. Potential quality evaluation matrix

### Experimental Matrix within buffers

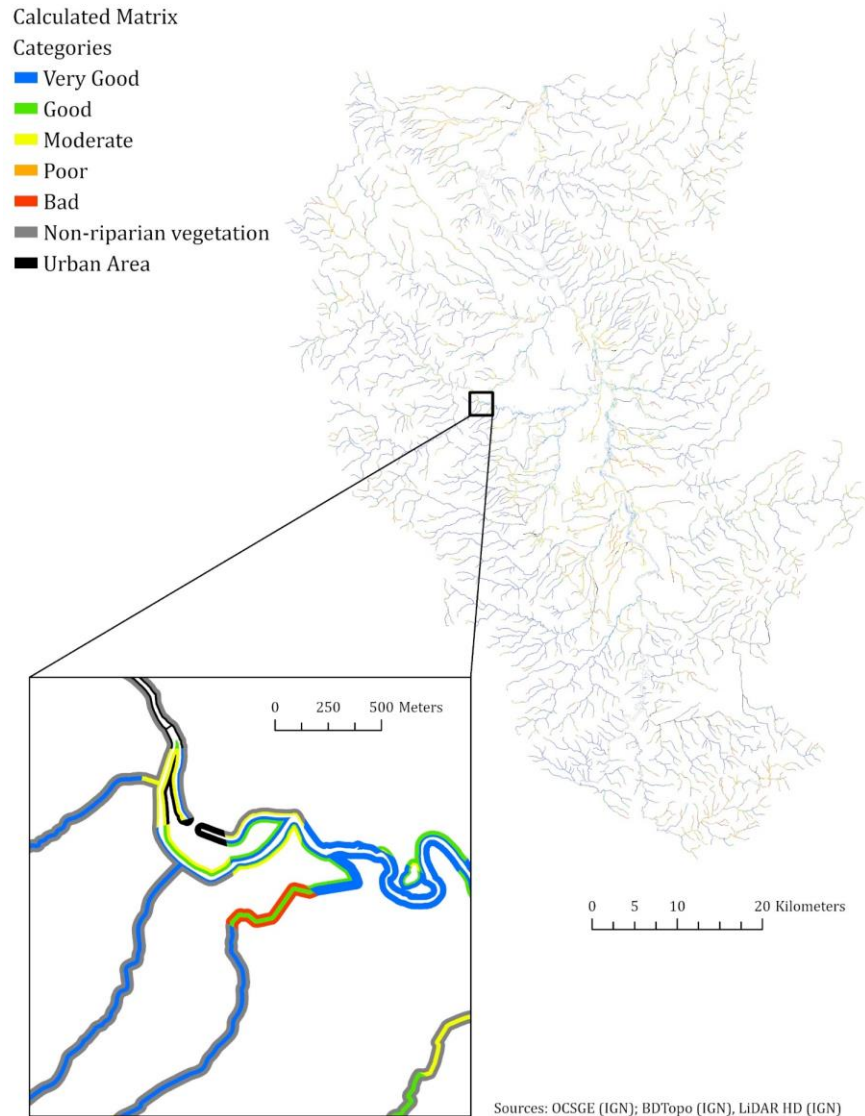


*Figure 13: Result of experimental buffer matrix, with a zoom on Boen sur Lignon*

This composite output synthesizes the results from buffer analyses by assigning qualitative classes (Very Good to Bad) to each buffer segment based on land use, vegetation coverage, and artificialization. Buffers closer to the watercourse were weighted more heavily, and scores were calculated to reflect degradation levels. The result identifies degraded zones requiring restoration and helps prioritize management actions. The method's spatial granularity ensures that even narrow or urban-impacted reaches are captured in the diagnostic. As this results are hard to read, a line-derived matrix was created



# Experimental Matrix

Calculated matrix over lines  
WFD-compliant categories

- Very Good
- Good
- Moderate
- Poor
- Bad
- No Data

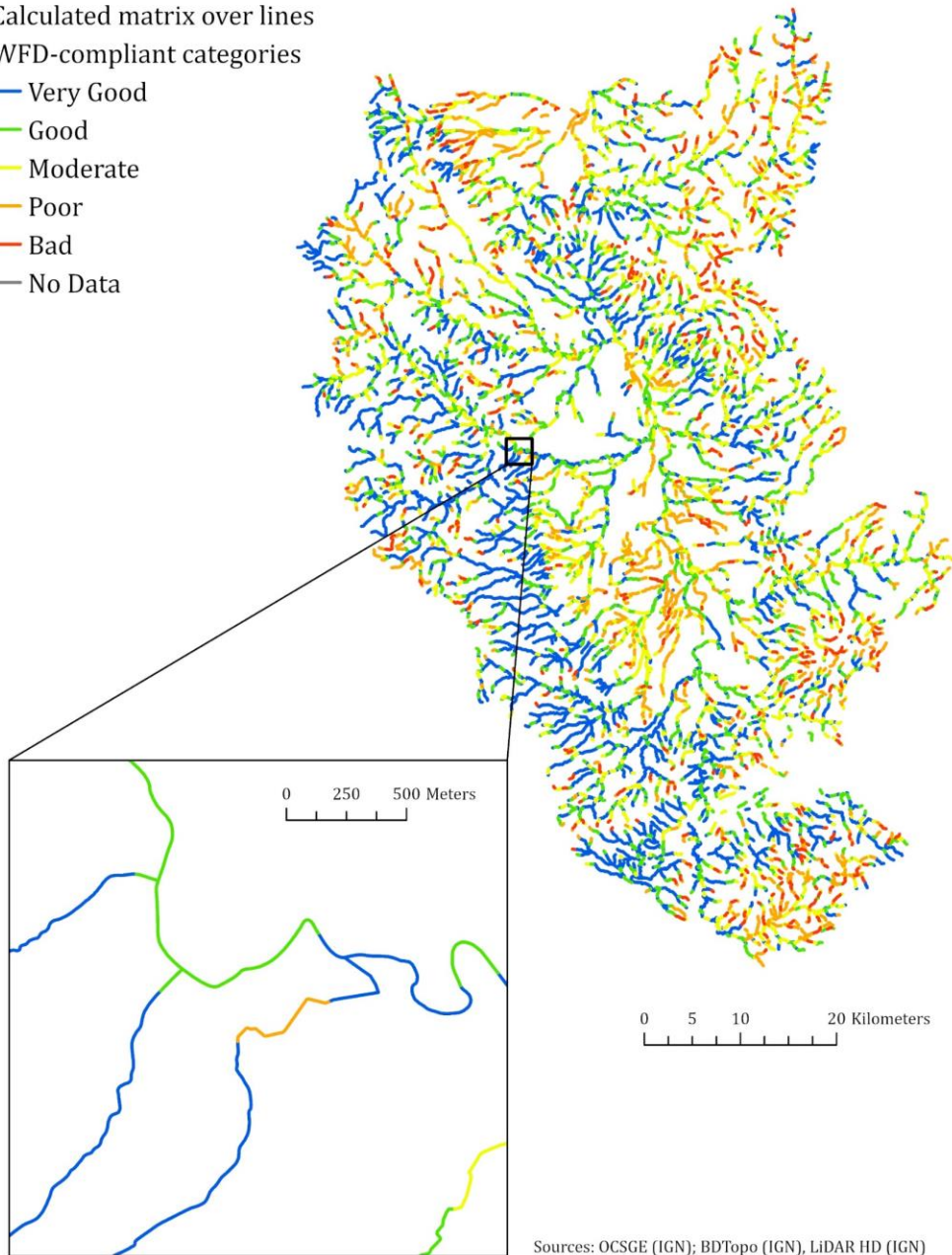


Figure 14: Result of the experimental matrix, displayed this time as lines, with a 500m reaches size, with a zoom on Boen sur Lignon.

Sources: OCSGE (IGN); BDTopo (IGN), LiDAR HD (IGN)

Using a weighted average of buffer scores, each 500 m reach of the hydrographic network was assigned a final qualitative class. This reach-scale synthesis transforms complex multi-buffer data into a readable management tool. Mapped results allow for a spatial overview of riparian condition across the watershed, aiding in restoration planning and stakeholder communication. The

classification algorithm, implemented as an automated ArcGIS tool, ensures repeatability and adaptability as new data becomes available.

All these results are available on a web map on the following link:

<https://univlyon2.maps.arcgis.com/apps/instant/basic/index.html?appid=cc367510753048e7b67e087b588816be>

## 9. Discussion

The integration of geomatics tools in the assessment of riparian vegetation within the *SAGE Loire en Rhône-Alpes* area has demonstrated the potential and the need of high-resolution remote sensing data to overcome the limitations of conventional datasets, even on very large datasets. Through a combination of LiDAR-derived vegetation mapping, DEM-based valley bottom delineation, continuity analysis, and composite scoring matrices, this study provides a spatially explicit, scalable framework for assessing riparian structure and ecological status.

One of the most important results concerns the mismatch between national-scale vegetation datasets and actual riparian forest presence (Figure 5). It illustrates the underrepresentation of small, fragmented, or linear vegetation features in traditional vector maps. Such discrepancies align with prior critiques on data granularity in national land cover products (Breton et al., 2023; Macfarlane et al., 2017), which often fail to detect smaller patches and very narrow corridors (one to two trees in width).

The valley bottom delineation provided ecogeomorphologically relevant zones of potential riparian presence. These methods, by incorporating parameters like valley slope, stream order, and flow accumulation thresholds, offer an improvement over fixed-distance buffer methods (Dufour et al., 2019; Gilbert et al., 2016), permitting to estimate where riparian vegetation should be present or not. However, their efficacy still depends on the resolution and hydrological accuracy of the underlying DEM. The use of GRASS GIS's *r.carve* function to correct anthropogenic interruptions in the DEM (e.g., bridges, culverts) and removing canals proved critical in ensuring hydrological coherence.

In terms of vegetation continuity, both longitudinal and lateral analyses revealed marked spatial heterogeneity. The longitudinal continuity map (Figure 10) underscored ruptures in riparian coverage, especially in agricultural and peri-urban zones—findings consistent with previous literature noting landscape fragmentation as a driver of ecosystem service loss (Riis et al., 2020). Lateral continuity analyses (Figure 12) further emphasized how buffer-based coverage diminishes with increasing distance from the riverbank, particularly beyond the 15-meter zone. This drop-off, while expected, quantifies the spatial limits of riparian influence and provides insight for management targets such as those set by the Ripascan or IBC-R indices.

The vegetation density results, derived from LiDAR point cloud classification, offered a structural proxy for riparian quality. While tools such as the *lidR* package in R enable tree segmentation and crown analysis, their efficacy in temperate, deciduous environments remains limited due to model calibration biases toward coniferous forests (Roussel et al., 2020). Attempts to use methods developed for evergreen forests proved to be complicated on deciduous forests. Many attempts were made in order to adjust the moving window, without completely covering the entirety of the trees presents.



The potential evaluation matrix methodology (Figures 13 and 14) demonstrated a functional approach to integrate multiple spatial indicators into a single index of riparian condition. By applying a weighted scoring system across three buffer zones per reach, and then translating these into reach-level classifications, this method provides a robust and scalable synthesis mechanism. The automation of this process through ArcGIS scripting ensures its replicability and adaptability to future datasets. However, it should be noted that while structural indicators such as vegetation presence and density are useful, the omission of functional ecological variables (e.g., shading capacity, biodiversity values, geomorphology features) may lead to over- or underestimation of ecological condition in certain contexts.

## 10. Limits

While this study presents a comprehensive framework for riparian vegetation mapping using high-resolution LiDAR, GIS analyses, and multi-buffered spatial assessments, several limitations need to be acknowledged. These limitations affect the interpretation, generalization, and future reproducibility of the results.

Despite the high spatial fidelity of LiDAR data, limitations in point density and classification accuracy can introduce uncertainties. In particular, areas under dense canopy or with heterogeneous land cover often present challenges for automated classification algorithms. While IGN's LiDAR HD dataset provides pre-classified returns, misclassification of features such as electricity pylons, hedgerows, or tall crops as high vegetation was occasionally observed. This issue has been highlighted in previous studies, where even advanced classification tools like the *lidR* R package can misinterpret vertical features, particularly in mixed or urbanized landscapes (Roussel et al., 2020; Stackhouse et al., 2023). The problem of temporal resolution of this data is also to pose. IGN released the LiDAR HD data from 2022, but there is no information on when the next one will be available.

The national vegetation datasets used for comparison (e.g., *Zone de Végétation*, OCS GE) are both either outdated and/or constrained by minimum mapping units (e.g., >5000 m<sup>2</sup>). These datasets fail to represent fine-scale, ecologically significant features, such as riparian hedgerows, scattered trees, or transitional forest zones. This limitation has already been widely recognized in the French context, where these databases often exclude riparian corridors less than 10 meters wide, despite their known ecological functions (Breton et al., 2023; Lochin et al., 2025).

Valley bottom delineation methods, depend heavily on the quality and resolution of the input DEMs. In areas with significant anthropogenic alterations—such as urban environments, bridge crossings, and levees—DEM hydrological flow paths may be inaccurate. Although corrective procedures (e.g., GRASS GIS's *r.carve*) were implemented to enforce hydrological connectivity, residual flow artifacts may still influence valley delineation outputs. This introduces spatial uncertainty into the ecological extent assumed for riparian development (Gilbert et al., 2016; Dufour et al., 2019).

The vegetation density proved to be inaccurate in some places and therefore does not appear on the evaluation matrix. The algorithm was capable to detect within a 20% error (compared visually with orthophotos), on a narrow riparian hedge, all the trees. However, as soon as the forested area was growing in area, the algorithm was underestimating by a factor 4.3 the number of trees. Therefore, this result is recurrent in the three sampled places across the *Lignon* River with the

formula used, which is not the case for the other formulas. For this task, deep learning models, trained on deciduous vegetation were also implemented, but with too much erroneous results to be considered.

The vegetation continuity metrics—both longitudinal and lateral—are reliant on the accuracy of vegetation masks derived from LiDAR. As such, any classification error in the base data will propagate through continuity analyses. Additionally, fixed buffer widths may not reflect ecologically meaningful distances for different stream sizes or riparian vegetation types, a limitation that has also been pointed out in international assessments (Macfarlane et al., 2018; Segura-Méndez et al., 2023).

The evaluation matrix approach, while robust in its aggregation of multiple buffer-level indicators, uses a discrete scoring system that may oversimplify ecological variability. By reducing riparian complexity to five ordinal classes (very good to bad), the method potentially masks intermediate conditions or fails to distinguish between structurally similar but functionally different riparian zones (Pace et al., 2022). Moreover, the use of fixed weights in the buffer zones assumes uniform importance across the study area, which may not account for geomorphological or land-use variability.

Lastly, the study's analytical framework is predominantly structural. It prioritizes measurable spatial and physical indicators (e.g., canopy height, coverage, proximity) and does not directly integrate functional or biological indicators, such as species richness, biomass productivity, or water quality buffering capacity. The absence of these variables means that the assessments may not fully capture the ecosystem services provided by riparian zones, nor their resilience to climate change and human pressures (Riis et al., 2020; Pace et al., 2022).

## 11. Perspectives

Building on the insights gained through this study, several key perspectives emerge to guide future research and applied management efforts in riparian vegetation monitoring and restoration. These perspectives span methodological refinements, integrative data strategies, participatory processes, and long-term ecological monitoring under climate and anthropogenic pressures.

One major area for advancement is the integration of functional ecological indicators alongside structural variables in riparian mapping workflows. While LiDAR and object-based classification provide robust data on vegetation height, canopy density, and spatial distribution, they fall short of capturing ecosystem functions such as nutrient retention, thermal buffering, or habitat suitability for specific taxa. Incorporating trait-based metrics (e.g., Ellenberg indicator values, Grime CSR strategies) could enhance ecological interpretation and support assessments of riparian condition beyond mere structure (Pace et al., 2022; Breton et al., 2023). The challenge remains to develop spatially explicit, standardized datasets of plant traits suitable for remote sensing integration, a research gap increasingly noted in functional ecology.

Second, there is considerable value in enhancing the temporal depth and continuity of monitoring frameworks. Riparian vegetation is highly dynamic, exhibiting seasonal and interannual fluctuations in response to hydrological regimes, disturbances, and succession processes. Yet most remote sensing analyses, including those in this study, rely on static imagery or single acquisition LiDAR. Emerging technologies such as UAV-based repeated monitoring, Sentinel-2 time series, or phenological modeling offer ways to track vegetation dynamics more responsively,

especially for restoration follow-up and climate resilience assessments (Lochin et al., 2024; Swetnam et al., 2018).

Another key perspective involves scaling up from local analyses to regional and national harmonization of methods. Current discrepancies in classification systems, buffer thresholds, and continuity metrics limit comparability between regions and projects (Segura-Méndez et al., 2023). The development of a shared typology or decision framework for riparian vegetation, similar to what is being piloted in programs like IBC-R, could support consistent data production across French catchments and inform national biodiversity and water policies. This also calls for improved interoperability of national datasets such as BD TOPO, OCS GE, and BD *Forêt*, which should evolve to better capture narrow, fragmented, or mixed riparian formations.

Participatory and transdisciplinary approaches also present a promising avenue for making riparian mapping more inclusive and action-oriented. While technically advanced outputs such as LiDAR-derived vegetation masks or buffer scoring matrices are valuable for researchers, they may not align with the decision-making needs of local managers or landowners. Co-production frameworks—where users co-define indicators, validate maps, and guide output visualization—can improve uptake, trust, and adaptability in planning contexts (Reed et al., 2014; Breton et al., 2023). Embedding geomatics outputs into tools such as online viewers, decision dashboards, or SAGE-specific planning portals could increase the practical relevance of your work.

Finally, the looming impacts of climate change and land-use transformation require a forward-looking integration of predictive modeling into riparian vegetation studies. Scenario-based approaches—combining spatial models of vegetation response with hydrological forecasts—can support anticipatory planning and restoration prioritization. Tools such as landscape connectivity models, species distribution modeling, or resilience-based planning frameworks are increasingly used in this context and could be adapted to the Loire region using your existing datasets (Riis et al., 2020; Godfroy et al., 2022).

## 12. Conclusion

This study developed and tested a spatially explicit methodology to characterize riparian vegetation at a large scale using geomatics tools, focusing on the SAGE *Loire en Rhône-Alpes* area. By combining LiDAR-based vegetation mapping, hydromorphological modeling, and spatial connectivity analyses, the project offers an integrative framework for identifying ecological patterns and anthropogenic pressures within riparian zones. The results demonstrate the effectiveness of combining valley bottom delineation with high-resolution vegetation data to detect and evaluate riparian integrity across diverse landscapes. Notably, the longitudinal and lateral connectivity assessments, along with the multi-buffer and reach-based evaluation matrices, enable nuanced classification of riparian condition across the study area.

While some technical limitations remain—such as incomplete LiDAR coverage, challenges in tree segmentation, and temporal mismatches between datasets—the methodology sets a foundation for replicability and further refinement. This approach contributes not only to research but also to practice, offering tangible tools for local decision-makers, especially under the scope of the SAGE's long-term water management objectives. Future work should prioritize field validation, functional trait integration, and temporal monitoring to strengthen ecological interpretations.

Ultimately, this internship supports the broader interdisciplinary cluster by operationalizing riparian assessment tools, aligning scientific inquiry with stakeholder needs, and fostering adaptive management under global change scenarios.

### 13. Acknowledgments

First, I want to thank my family for always being there for me throughout this master's year. Your support, encouragement, and patience meant a lot, especially during the more intense moments.

A big thanks to my friends as well—for the laughs, the motivation, and the breaks I definitely needed. You helped keep things in balance.

A very big thanks to my co-internship cluster friends, who made field trips a real pleasure, even if we had to endure being trapped in sediments or cross three times the entire study area.

I'm really grateful to Pierre-Olivier Mazagol for his constant support and guidance during my internship. Your feedback and availability made a real difference in how this project came together.

I want to thank as well Amélie Potignon, at the SAGE *Loire en Rhone Alpes*, for her responsiveness and her availability throughout this internship.

A warm thank you to everyone at EVS-ISTHME in Saint-Étienne. The many insightful conversations—whether during lunchtime or around a coffee—really helped shape my thinking and made this experience both enriching and enjoyable.

Last but not least, a very big thank to Alyssa, Claire-Lise, Elisabeth and Marina at the EUR H2O for their time and their impeccable organization skills.

## 14. References

- Baatrup-Pedersen, A., Garssen, A., Göthe, E., Hoffmann, C. C., Oddershede, A., Riis, T., Van Bodegom, P. M., Larsen, S. E., & Soons, M. (2018). Structural and functional responses of plant communities to climate change-mediated alterations in the hydrology of riparian areas in temperate Europe. *Ecology and Evolution*, 8(8), 4120–4135. <https://doi.org/10.1002/ece3.3973>
- Boudrie, M. (2004). Présentation géologique de l'ensemble Monts du Forez, montagne Bourbonnaise, limagnes, plaine du Forez. *Le Journal de botanique*, 26(1), 57–59. <https://doi.org/10.3406/jobot.2004.2069>
- Breton, V., Girel, J., & Janssen, P. (2023). Long-term changes in the riparian vegetation of a large, highly anthropized river: Towards less hygrophilous and more competitive communities. *Ecological Indicators*, 155, 111015. <https://doi.org/10.1016/j.ecolind.2023.111015>
- Camporeale, C., Perucca, E., Ridolfi, L., & Gurnell, A. M. (2013). Modeling the interactions between river morphodynamics and riparian vegetation. *Reviews of Geophysics*, 51(3), 379–414. <https://doi.org/10.1002/rog.20014>
- Capon, S. J., Chambers, L. E., Mac Nally, R., Naiman, R. J., Davies, P., Marshall, N., Pittock, J., Reid, M., Capon, T., Douglas, M., Catford, J., Baldwin, D. S., Stewardson, M., Roberts, J., Parsons, M., & Williams, S. E. (2013). Riparian Ecosystems in the 21st Century: Hotspots for Climate Change Adaptation? *Ecosystems*, 16(3), 359–381. <https://doi.org/10.1007/s10021-013-9656-1>
- Clubb, F. J., Mudd, S. M., Milodowski, D. T., Valters, D. A., Slater, L. J., Hurst, M. D., & Limaye, A. B. (2017). Geomorphometric delineation of floodplains and terraces from objectively defined topographic thresholds. *Earth Surface Dynamics*, 5(3), 369–385. <https://doi.org/10.5194/esurf-5-369-2017>
- Cvitanovic, C., McDonald, J., & Hobday, A. J. (2016). From science to action: Principles for undertaking environmental research that enables knowledge exchange and evidence-based decision-making. *Journal of Environmental Management*, 183, 864–874. <https://doi.org/10.1016/j.jenvman.2016.09.038>
- Danielsen, F., Pirhofer-Walzl, K., Adrian, T. P., Kapijimpanga, D. R., Burgess, N. D., Jensen, P. M., Bonney, R., Funder, M., Landa, A., Levermann, N., & Madsen, J. (2014). Linking Public Participation in Scientific Research to the Indicators and Needs of International Environmental Agreements. *Conservation Letters*, 7(1), 12–24. <https://doi.org/10.1111/conl.12024>
- Dufour, S., Rodriguez-Gonzalez, P. M., & Laslier, M. (2019). Tracing the scientific trajectory of riparian vegetation studies: Main topics, approaches and needs in a globally changing world. *Science of The Total Environment*, 653, 1168–1185. <https://doi.org/10.1016/j.scitotenv.2018.10.383>
- EPTB Loire. (n.d.). Adaptation aux impacts du changement climatique. *Etablissement Public Loire*. Retrieved June 2, 2025, from <https://www.eptb-loire.fr/nos-missions/recherche-developpement-et-innovation/adaptation-aux-impacts-du-changement-climatique-2/>
- European Parliament. (2000). *Directive—2000/60—EN - Water Framework Directive—EUR-Lex*. <https://eur-lex.europa.eu/eli/dir/2000/60/oj/eng>
- European Union. (2024). *EU Nature Restoration Law*. [https://environment.ec.europa.eu/topics/nature-and-biodiversity/nature-restoration-law\\_en](https://environment.ec.europa.eu/topics/nature-and-biodiversity/nature-restoration-law_en)

- Faure, M., Bé Mézème, E., Duguet, M., Cartier, C., & Talbot, J.-Y. (2005). Paleozoic tectonic evolution of medio-Europa from the example of the French Massif Central and Massif Armoricain. *Journal of the Virtual Explorer*, 19. <https://doi.org/10.3809/jvirtex.2005.00120>
- Fazey, I., Bunse, L., Msika, J., Pinke, M., Preedy, K., Evely, A. C., Lambert, E., Hastings, E., Morris, S., & Reed, M. S. (2014). Evaluating knowledge exchange in interdisciplinary and multi-stakeholder research. *Global Environmental Change*, 25, 204–220. <https://doi.org/10.1016/j.gloenvcha.2013.12.012>
- Galtier, J., & Guillerme, N. (2004). La plaine du Forez. *Le Journal de botanique*, 26(1), 61–66. <https://doi.org/10.3406/jobot.2004.2070>
- Gilbert, J. T., Macfarlane, W. W., & Wheaton, J. M. (2016). The Valley Bottom Extraction Tool (V-BET): A GIS tool for delineating valley bottoms across entire drainage networks. *Computers & Geosciences*, 97, 1–14. <https://doi.org/10.1016/j.cageo.2016.07.014>
- Glossaire eau et biodiversité. (2018). *Ripisylve Definition*. Glossaire eau, milieu marin et biodiversité. <https://glossaire.eauetbiodiversite.fr/concept/ripisylve>
- Godfroy, J., Lejot, J., Demarchi, L., Bizzi, S., Michel, K., & Piégay, H. (2022). Combining Hyperspectral, LiDAR, and Forestry Data to Characterize Riparian Forests along Age and Hydrological Gradients. *Remote Sensing*, 15(1), 17. <https://doi.org/10.3390/rs15010017>
- Grijseels, N. H., Buchert, M., Brooks, P. D., & Pataki, D. E. (2021). Using LiDAR to assess transitions in riparian vegetation structure along a rural-to-urban land use gradient in western North America. *Ecohydrology*, 14(1), e2259. <https://doi.org/10.1002/eco.2259>
- Janssen, P., Evette, A., Bergès, L., Gonin, P., Larrieu, L., Dajoux, M., Dupont, S., Gardien, S., Gilles, C., & Ladet, A. (2021). Évaluer la qualité des boisements riverains avec l'Indice de Biodiversité et de Connectivité des Ripisylves (IBCR): Une étude de cas avec les communautés d'oiseaux. *Naturae*, 21. <https://doi.org/10.5852/naturae2021a21>
- Lejot, J., Piégay, H., Hunter, P. David., Moulin, B., & Gagnage, M. (2011). Utilisation de la télédétection pour la caractérisation des corridors fluviaux: Exemples d'applications et enjeux actuels. *Géomorphologie : Relief, Processus, Environnement*, 17(2), 157–172. <https://doi.org/10.4000/geomorphologie.9362>
- Lochin, P., Piégay, H., Stella, J. C., Caylor, K. K., Vaudor, L., & Bliss Singer, M. (2025). Drivers of Spatiotemporal Patterns of Riparian Forest NDVI Along a Hydroclimatic Gradient. *Ecohydrology*, 18(2), e2729. <https://doi.org/10.1002/eco.2729>
- Macfarlane, W. W., Gilbert, J. T., Jensen, M. L., Gilbert, J. D., Hough-Snee, N., McHugh, P. A., Wheaton, J. M., & Bennett, S. N. (2017). Riparian vegetation as an indicator of riparian condition: Detecting departures from historic condition across the North American West. *Journal of Environmental Management*, 202, 447–460. <https://doi.org/10.1016/j.jenvman.2016.10.054>
- Mc Donald, D., de Billy, V., & Georges, N. (2018). *Bonnes pratiques environnementales. Cas de la protection des milieux aquatiques en phase chantier: Anticipation des risques, gestion des sédiments et autres sources potentielles de pollutions des eaux*. Collection Guides et protocoles.
- Metz, M., Egger, G., Díaz-Redondo, M., Garófano Gómez, V., Hortobágyi, B., Steiger, J., & Corenblit, D. (2016). *Succession processes of a dynamic riparian ecosystem: The lower Allier River (France)*.
- Michez, A., Piégay, H., Lejeune, P., & Claessens, H. (2017). Multi-temporal monitoring of a regional riparian buffer network (>12,000 km) with LiDAR and photogrammetric point

- clouds. *Journal of Environmental Management*, 202, 424–436. <https://doi.org/10.1016/j.jenvman.2017.02.034>
- Monnet, J.-M. (2010). *Tree top detection using local maxima filtering: A parameter sensitivity analysis*.
- Naiman, R. J., Decamps, H., & Pollock, M. (1993). The Role of Riparian Corridors in Maintaining Regional Biodiversity. *Ecological Applications*, 3(2), 209–212. <https://doi.org/10.2307/1941822>
- Pace, G., Gutiérrez-Cánovas, C., Henriques, R., Carvalho-Santos, C., Cássio, F., & Pascoal, C. (2022). Remote sensing indicators to assess riparian vegetation and river ecosystem health. *Ecological Indicators*, 144, 109519. <https://doi.org/10.1016/j.ecolind.2022.109519>
- Piégay, H., Darby, S. E., Mosselman, E., & Surian, N. (2005). A review of techniques available for delimiting the erodible river corridor: A sustainable approach to managing bank erosion. *River Research and Applications*, 21(7), 773–789. <https://doi.org/10.1002/rra.881>
- Pitkänen, J., Maltamo, M., Hyypä, J., & Yu, X. (2001). *Adaptive methods for individual tree detection on airborne laser based canopy height model*.
- Popescu, S. C., & Wynne, R. H. (2004). *Seeing the Trees in the Forest: Using Lidar and Multispectral Data Fusion with Local Filtering and Variable Window Size for Estimating Tree Height*.
- Quenardel, J.-M., Santallier, D., Burg, J.-P., Bril, H., Cathelineau, M., & Marignac, C. (1991). Le Massif Central / The central massif. *Sciences Géologiques. Bulletin*, 44(1), 105–206. <https://doi.org/10.3406/sgeol.1991.1866>
- Reed, M. S., Stringer, L. C., Fazey, I., Evely, A. C., & Kruijsen, J. H. J. (2014). Five principles for the practice of knowledge exchange in environmental management. *Journal of Environmental Management*, 146, 337–345. <https://doi.org/10.1016/j.jenvman.2014.07.021>
- Riis, T., Kelly-Quinn, M., Aguiar, F. C., Manolaki, P., Bruno, D., Bejarano, M. D., Clerici, N., Fernandes, M. R., Franco, J. C., Pettit, N., Portela, A. P., Tammeorg, O., Tammeorg, P., Rodríguez-González, P. M., & Dufour, S. (2020). Global Overview of Ecosystem Services Provided by Riparian Vegetation. *BioScience*, 70(6), 501–514. <https://doi.org/10.1093/biosci/biaa041>
- Roussel, J.-R., Auty, D., Coops, N. C., Tompalski, P., Goodbody, T. R. H., Meador, A. S., Bourdon, J.-F., De Boissieu, F., & Achim, A. (2020). lidR: An R package for analysis of Airborne Laser Scanning (ALS) data. *Remote Sensing of Environment*, 251, 112061. <https://doi.org/10.1016/j.rse.2020.112061>
- Roux, C., Alber, A., Bertrand, M., Vaudor, L., & Piégay, H. (2015). “Fluvial Corridor”: A new ArcGis Toolbox Package for multiscale riverscape exploration. *Geomorphology*, 242, 29–37.
- SAGE LRA. (2014). *Plan d’aménagement et de gestion durable*. <https://sage-loire-rhone-alpes.fr/wp-content/uploads/2024/08/PAGD.pdf>
- Sciuto, L., Licciardello, F., Barbera, A. C., & Cirelli, G. (2022). A GIS-based multicriteria decision analysis to reduce riparian vegetation hydrogeological risk and to quantify harvested biomass (Giant reed) for energetic retrieval. *Ecological Indicators*, 144, 109548. <https://doi.org/10.1016/j.ecolind.2022.109548>
- Seavy, N. E., Gardali, T., Golet, G. H., Griggs, F. T., Howell, C. A., Kelsey, R., Small, S. L., Viers, J. H., & Weigand, J. F. (2009). Why Climate Change Makes Riparian Restoration More

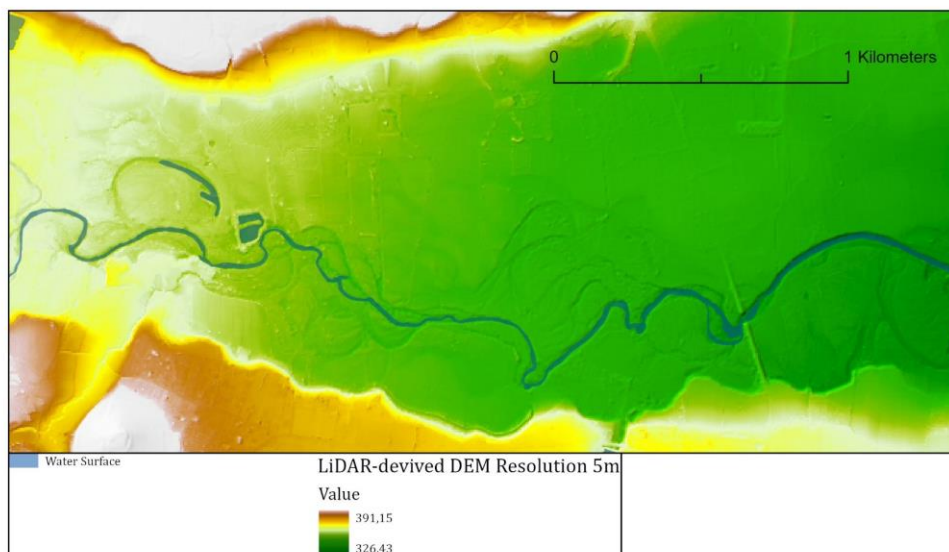
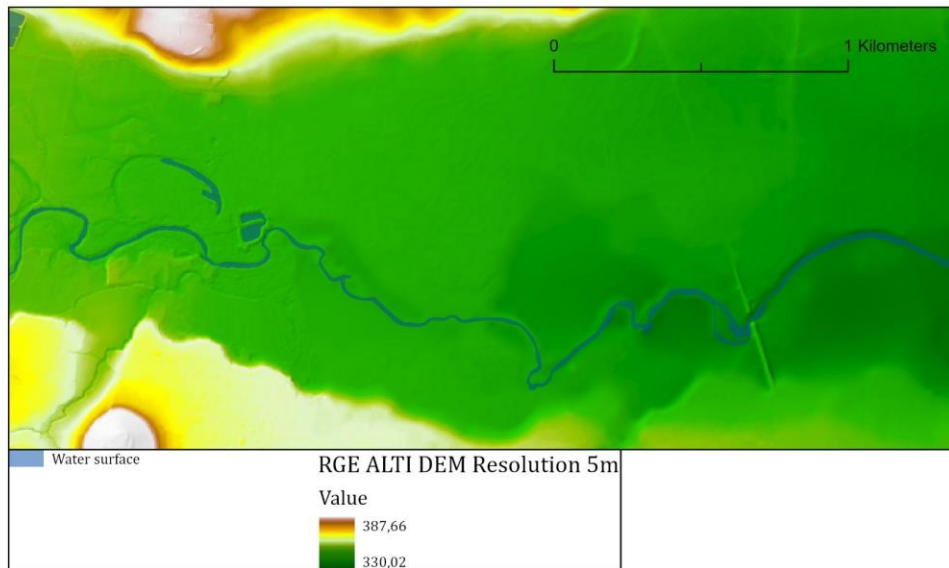
- Important than Ever: Recommendations for Practice and Research. *Ecological Restoration*, 27(3), 330–338. <https://doi.org/10.3368/er.27.3.330>
- Segura-Méndez, F. J., Pérez-Sánchez, J., & Senent-Aparicio, J. (2023). Evaluating the riparian forest quality index (QBR) in the Luchena River by integrating remote sensing, machine learning and GIS techniques. *Ecohydrology & Hydrobiology*, 23(3), 469–483. <https://doi.org/10.1016/j.ecohyd.2023.04.002>
- Soille, P., Vogt, J., & Colombo, R. (2003). Carving and adaptive drainage enforcement of grid digital elevation models. *Water Resources Research*, 39(12), 2002WR001879. <https://doi.org/10.1029/2002WR001879>
- Stackhouse, L. A., Coops, N. C., White, J. C., Tompalski, P., Hamilton, J., & Davis, D. J. (2023). Characterizing riparian vegetation and classifying riparian extent using airborne laser scanning data. *Ecological Indicators*, 152, 110366. <https://doi.org/10.1016/j.ecolind.2023.110366>
- Staentzel, C. (2025, February 4). *RipaScan*. RipaScan. <https://ripascan.org/>
- Stella, J. C., Rodríguez-González, P. M., Dufour, S., & Bendix, J. (2013). Riparian vegetation research in Mediterranean-climate regions: Common patterns, ecological processes, and considerations for management. *Hydrobiologia*, 719(1), 291–315. <https://doi.org/10.1007/s10750-012-1304-9>
- Sweeney, B. W., & Newbold, J. D. (2014). Streamside Forest Buffer Width Needed to Protect Stream Water Quality, Habitat, and Organisms: A Literature Review. *JAWRA Journal of the American Water Resources Association*, 50(3), 560–584. <https://doi.org/10.1111/jawr.12203>
- Vitel, G. (with Centre d'études foréziennes). (2001). *Géologie de la Loire: Invitation à la lecture des paysages*. Publications de l'Université de Saint-Étienne.



## 15. Appendix

### 15.1. Appendix 1: DEM Detail

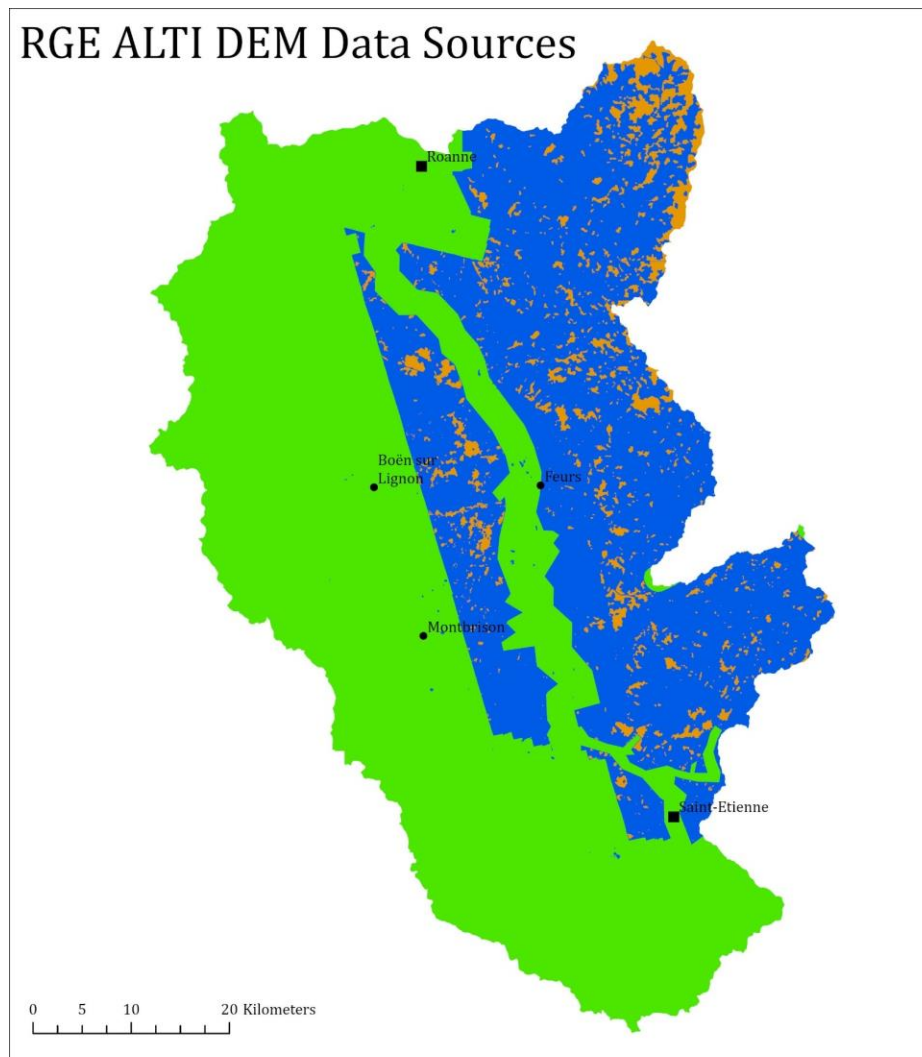
Detail difference between the RGE ALTI and LiDAR-derived DEM near La Bathie d'Urfé (Lignon River)



Sources: OCSGE (IGN); RGE ALTI (IGN); LiDAR HD (IGN)

*Appendix 1: Difference between available RGE ALTI DEM and LiDAR-derived DEM*

## 15.2. Appendix 2 : RGE Alti DEM Data Sources



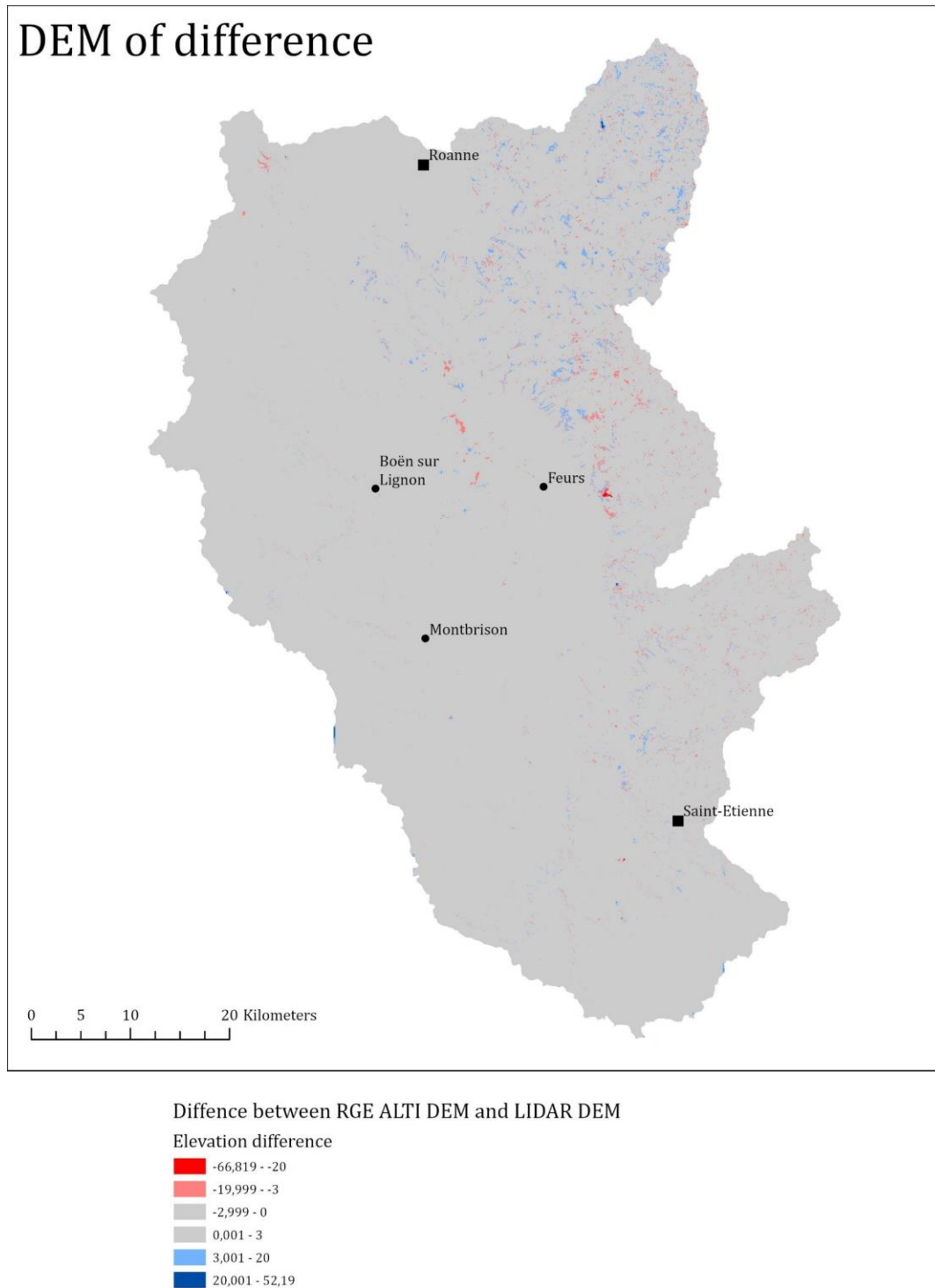
### RGE ALTI Data Sources

#### ORIGIN

- BD ALTI
- LiDAR (Topography and/or Bathymetry)
- Winter photogrammetry

*Appendix 2: REG ALTI DEM data sources over the study area, showing re-sampled 25m resolution BD ALTI, low resolution lidar data, and winter photogrammetry..*

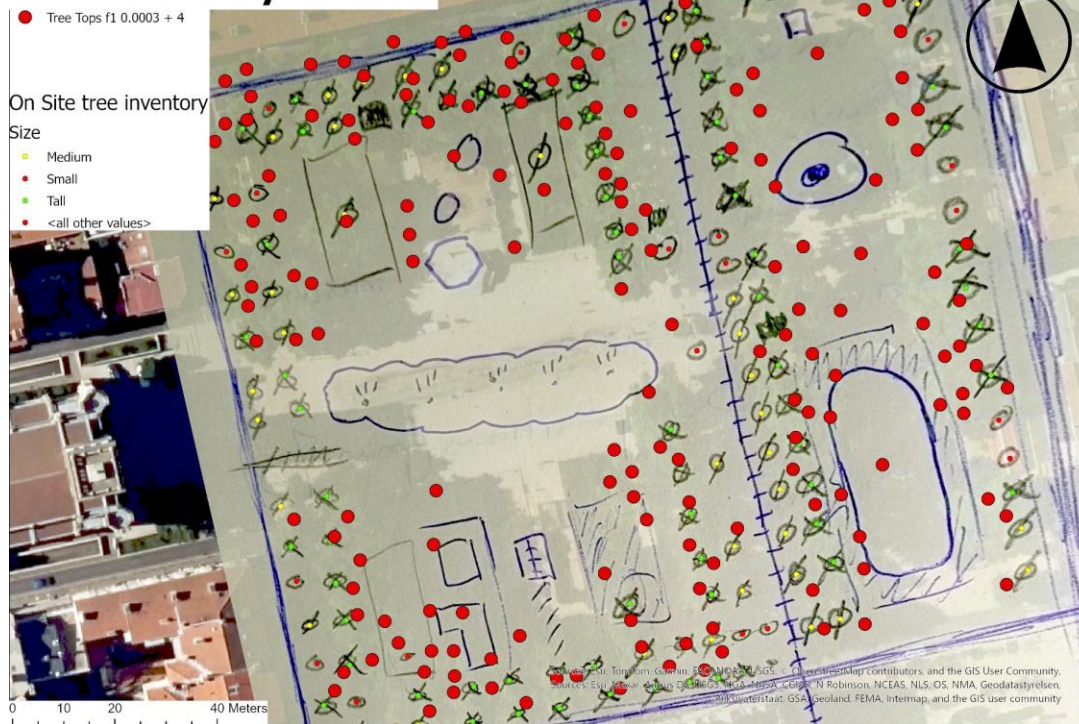
### 15.3. Appendix 3: DEM of Difference between LiDAR and RGE Alti



*Appendix 3: DEM of Difference between the RGE ALTI and the LiDAR-derived DEM*

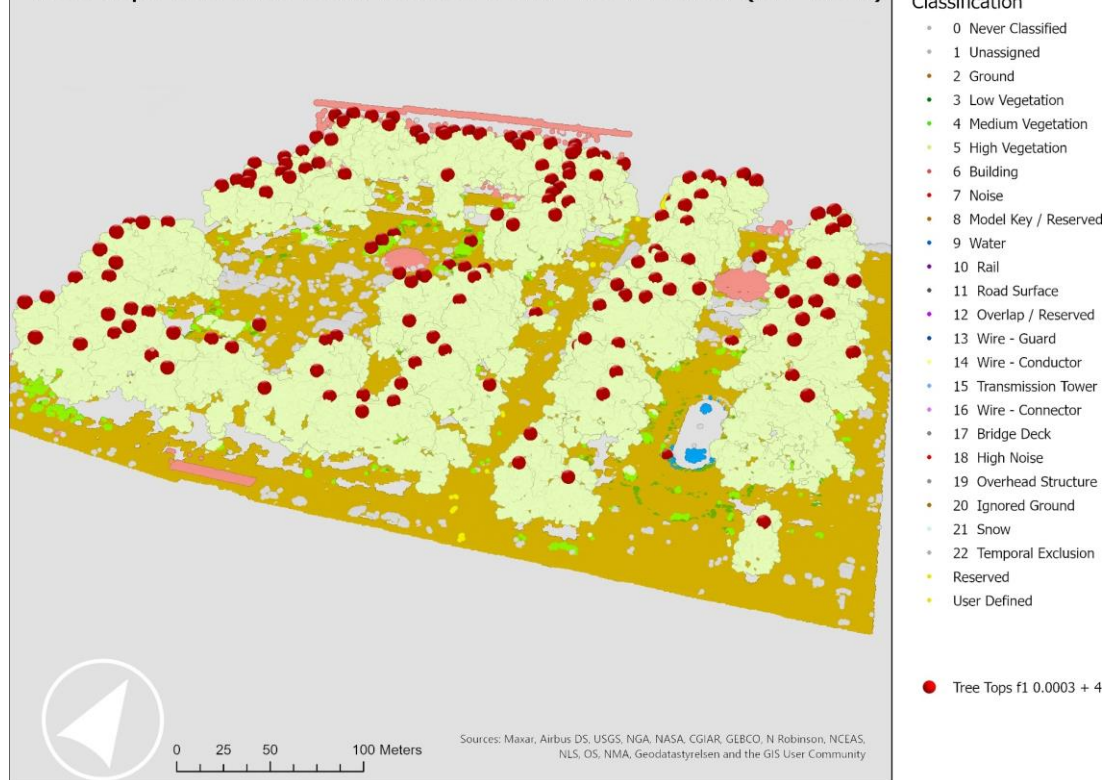
#### 15.4. Appendix 4: In situ validation for vegetation density

## Tree Inventory on site



Appendix 5: Geolocalised tree count on site in Saint Etienne, compared with the detected trees with the best formula.

### Tree tops at Place Jean-Jaures from LiDAR Data (3D view)



Appendix 4: 3D view of the place Jean-Jaures in Saint Etienne, used for calibration of the algorithm, with results with the best formula



## 15.5. Appendix 4: R script: DEM from LiDAR

```
1. # =====
2. # Create 5m DEM from LiDAR Tiles (Class 2 & 9)
3. # Class 2 and 9 are respectively Ground and Water (to have a more coherent water surface)
4. # =====
5.
6. # Clear workspace
7. rm(list = ls())
8.
9. # Load required libraries
10. library(lidR)
11. library(raster)
12. library(future)
13. library(terra) # Load terra explicitly for SpatRaster support
14.
15.
16.
17. # Enable multiprocessing
18. plan(multisession, workers = parallel::detectCores())
19.
20. # Paths
21. las_folder <- "C://your_folder" # Folder with LAS/LAZ tiles
22. output_dtm_path <- "C://output_folder//merged_dtm_5m.tif" # Output GeoTIFF path
23.
24. # Load LAS catalog
25. ctg <- readLAScatalog(las_folder)
26.
27. # Catalog options
28. opt_chunk_buffer(ctg) <- 0
29. opt_independent_files(ctg) <- TRUE
30. opt_progress(ctg) <- TRUE
31.
32. # Set output resolution (in meters)
33. dtm_resolution <- 5
34.
35. # Create DTM using classes 2 (ground) and 9 (water)
36. dtm <- rasterize_terrain(
37.   ctg,
38.   algorithm = tin(), # You can also try kriging(k = 10) or knnidw(k = 10)
39.   res = dtm_resolution,
40.   filter = "-keep_class 2 9"
41. )
42.
43. # Save as a single GeoTIFF
44. writeRaster(dtm, output_dtm_path, filetype = "GTiff", overwrite = TRUE)
45.
46. cat("\n DTM generation complete.\nSaved to:", output_dtm_path, "\n")
47.
```

*Appendix 6: R script for batch DEM creation from LiDAR data*

## 15.6. Appendix 5: R script: Tree top extraction

```
1. # =====
2. # Tree Top detection from LiDAR tiles - Class 5 (High Vegetation Only)
3. # It will create one Shapefile per tile and one merged Shapefile at the end of the process
4. # =====
5.
6. # Clear environment
7. rm(list = ls(globalenv()))
8.
9. # Load Libraries
10. library(lidR)
11. library(sf)
12. library(tools)
13. library(future)
14.
15. # Parallel setup: All cores
16. plan(multisession, workers = parallel::detectCores())
17.
18. # Start timer
19. start_time <- Sys.time()
20.
21. # Paths
22. las_folder <- "C://your_folder" # Folder with LAS/LAZ tiles
23. output_folder <- "C://output_folder//x003_4" # Output folder
24. dir.create(output_folder, showWarnings = FALSE, recursive = TRUE)
25.
26. # Define the detection function
27. f <- function(x) { x * 0.003 + 4 }
28. fname <- "x003_4"
29.
30. # Load catalog
31. las_catalog <- readLAScatalog(las_folder)
32.
33. # Catalog options
34. opt_chunk_buffer(las_catalog) <- 0
35. opt_independent_files(las_catalog) <- TRUE
36. opt_progress(las_catalog) <- TRUE
37.
38. # Processing function for catalog_apply
39. process_tile <- function(cluster) {
40.   las <- readLAS(cluster, filter = "-keep_class 5 -set_withheld_flag 0")
41.   if (is.null(las) || nrow(las) == 0) return(NULL)
42.
43.   tile_name <- file_path_sans_ext(basename(attr(cluster, "file")))
44.   cat("Processing tile:", tile_name, "\n")
45.
46.   # Tree detection
47.   ttops <- locate_trees(las, lmf(f))
48.
49.   if (!is.null(ttops) && nrow(ttops) > 0) {
50.     out_file <- file.path(output_folder, paste0("tree_tops_", fname, "_", tile_name, ".shp"))
51.
52.     st_write(ttops, dsn = out_file, driver = "ESRI Shapefile",
53.               layer_options = "SHPT=POINTZ", delete_layer = TRUE)
54.   }
55.
56.   return(NULL)
57. }
58.
59. # Apply to catalog
60. catalog_apply(las_catalog, process_tile)
```



```

61.
62. # --- Merge outputs
63. cat("Merging shapefiles...\n")
64. shapefiles <- list.files(output_folder, pattern = "\\..shp$", full.names = TRUE)
65. shapes_list <- lapply(shapefiles, st_read, quiet = TRUE)
66.
67. merged_count <- 0
68. if (length(shapes_list) > 0) {
69.   merged_shapes <- do.call(rbind, shapes_list)
70.   merged_file <- file.path(output_folder, paste0("merged_tree_tops_", fname, ".shp"))
71.   st_write(merged_shapes, merged_file, driver = "ESRI Shapefile",
72.     layer_options = "SHPT=POINTZ", delete_layer = TRUE)
73.   merged_count <- nrow(merged_shapes)
74. }
75.
76. # --- Timing
77. end_time <- Sys.time()
78. processing_time <- end_time - start_time
79. hours <- as.integer(processing_time / 3600)
80. minutes <- as.integer((processing_time * 3600) / 60)
81. seconds <- round(processing_time * 60, 2)
82.
83. # --- Write summary
84. output_txt <- file.path(output_folder, paste0("Process_Summary_", format(end_time,
"%Y_%m_%d_%H_%M"), ".txt"))
85. sink(output_txt)
86.
87. cat("Tree Top Detection Process Summary\n")
88. cat("=====\n")
89. cat("Filtered only Class 5 (high vegetation) points\n\n")
90. cat(sprintf("Total number of tiles processed: %d\n", length(las_catalog)))
91. cat(sprintf("Total processing time: %02d:%02d:%05.2f (HH:MM:SS)\n\n", hours, minutes, seconds))
92. cat(sprintf("Function %s → Total Trees Detected: %d\n", fname, merged_count))
93.
94. sink() # Close text file
95.
96. cat("\n Processing complete. Outputs saved in:", output_folder, "\n")
97.

```

*Appendix 7: R script for the batch Tree Top detection using LiDAR*

## 15.7. Appendix 6: Python scripts for the evaluation matrix

```
1. import arcpy
2.
3. def degradation_driver(forest, vb, built):
4.     if vb in ["Moderate", "Poor", "Bad"]:
5.         return "Non-riparian vegetation"
6.     if built in ["Poor", "Bad"]:
7.         return "Urban Area"
8.
9.     rank = {"Very Good": 5, "Good": 4, "Moderate": 3, "Poor": 2, "Bad": 1}
10.    reverse_rank = {v: k for k, v in rank.items()}
11.
12.    scores = {
13.        "Forest_Qual": rank.get(forest, 0),
14.        "VB_Qual": rank.get(vb, 0),
15.        "Built_Qual": rank.get(built, 0)
16.    }
17.
18.    # Find the lowest ranking value (most degrading) and return its qualitative label
19.    lowest_score = min(scores.values())
20.    return reverse_rank.get(lowest_score, "Unknown")
21.
22. def main():
23.     arcpy.env.overwriteOutput = True
24.
25.     input_fc = arcpy.GetParameterAsText(0) # Input feature class
26.     output_field = arcpy.GetParameterAsText(1) # Output field name
27.
28.     # Check if output field exists, if not create it
29.     field_names = [f.name for f in arcpy.ListFields(input_fc)]
30.     if output_field not in field_names:
31.         arcpy.AddMessage(f"Creating new field: {output_field}")
32.         arcpy.AddField_management(input_fc, output_field, "TEXT", field_length=50)
33.
34.     with arcpy.da.UpdateCursor(input_fc, ["Forest_Qual", "VB_Qual", "Built_Qual", output_field])
as cursor:
35.         for row in cursor:
36.             forest, vb, built = row[0], row[1], row[2]
37.             row[3] = degradation_driver(forest, vb, built)
38.             cursor.updateRow(row)
39.
40.     arcpy.AddMessage("Degradation evaluation completed.")
41.
42. if __name__ == '__main__':
43.     main()
44.
```

*Appendix 8: Python script used to create the buffered evaluation matrix.*

```

1. import arcpy
2. from collections import defaultdict
3.
4. def classify_score(score):
5.     if score >= 4.5:
6.         return "Very Good"
7.     elif score >= 3.5:
8.         return "Good"
9.     elif score >= 2.5:
10.        return "Moderate"
11.    elif score >= 1.5:
12.        return "Poor"
13.    else:
14.        return "Bad"
15.
16. def main():
17.     arcpy.env.overwriteOutput = True
18.
19.     buffer_fc = arcpy.GetParameterAsText(0) # Input buffer polygons with 'ID', 'Matrix',
'ID_BUFFER'
20.     reach_fc = arcpy.GetParameterAsText(1) # Input line layer with 'ReachID'
21.     output_field = arcpy.GetParameterAsText(2) # Output field name for qualitative score
22.
23.     # Mapping from qualitative labels to scores
24.     qual_to_score = {
25.         "Very Good": 5,
26.         "Good": 4,
27.         "Moderate": 3,
28.         "Poor": 2,
29.         "Bad": 1
30.         # Exclude "Urban Area" and "Non-riparian vegetation"
31.     }
32.     weight_map = {1: 3, 2: 2, 3: 1} # Higher weight for more important buffers
33.
34.     # Aggregate scores from buffer features by ID
35.     scores_by_id = defaultdict(lambda: {"total": 0, "weight": 0})
36.     with arcpy.da.SearchCursor(buffer_fc, ["ID", "Matrix", "ID_BUFFER"]) as cursor:
37.         for rid, matrix, buff in cursor:
38.             if rid is None or matrix is None or buff is None:
39.                 continue # Skip incomplete records
40.             if matrix in ["Urban Area", "Non-riparian vegetation"]:
41.                 continue # Exclude irrelevant classifications
42.             try:
43.                 rid_str = str(int(float(rid)))
44.             except (ValueError, TypeError):
45.                 continue # Skip if ID can't be converted
46.             if matrix in qual_to_score and buff in weight_map:
47.                 score = qual_to_score[matrix]
48.                 weight = weight_map[buff]
49.                 scores_by_id[rid_str]["total"] += score * weight
50.                 scores_by_id[rid_str]["weight"] += weight
51.
52.     # Add output field to reach_fc if it doesn't exist
53.     field_names = [f.name for f in arcpy.ListFields(reach_fc)]
54.     if output_field not in field_names:
55.         arcpy.AddMessage(f"Creating new field: {output_field}")
56.         arcpy.AddField_management(reach_fc, output_field, "TEXT", field_length=20)
57.
58.     # Update reach features with classified scores
59.     with arcpy.da.UpdateCursor(reach_fc, ["ReachID", output_field]) as cursor:
60.         for row in cursor:
61.             rid = str(row[0])
62.             if rid in scores_by_id and scores_by_id[rid]["weight"] > 0:
63.                 avg_score = scores_by_id[rid]["total"] / scores_by_id[rid]["weight"]
64.                 row[1] = classify_score(avg_score)

```

```
65.             cursor.updateRow(row)
66.
67.     arcpy.AddMessage("Weighted classification from buffer layer applied to line features.")
68.
69. if __name__ == '__main__':
70.     main()
71.
```

*Appendix 9: Python script used to merge the buffered result to a line result.*